Signatures of the Madden-Julian Oscillation in Middle Atmosphere zonal mean Temperature: Triggering the Interhemispheric Coupling pattern

Christoph G. Hoffmann[1], Lena G. Buth[1,2], and Christian von Savigny[1]

[1]Institute of Physics, University of Greifswald, Felix-Hausdorff-Str. 6, 17489 Greifswald, Germany
[2]now at Alfred Wegener Institute, Helmholtz Centre for Polar and Marine Research, Bremerhaven, Germany

Correspondence: Christoph G. Hoffmann (christoph.hoffmann@uni-greifswald.de)

Abstract. The influence of the Madden–Julian oscillation (MJO) on the middle atmosphere (MA) and particularly on MA temperature is of interest for both the understanding of MJO-induced teleconnections and research on the variability of the MA. We analyze statistically the connection of the MJO and the MA zonal mean temperature based on observations by the MLS satellite instrument. We consider all eight MJO phases, different seasons and the state of the quasi-biennial oscillation (QBO). We show that the MA temperature ~~is influenced by the state of MJO in large areas of the MA and under roughly all considered atmospheric conditions. The zonal mean temperature response shows~~ anomalies are significantly related to the MJO and its temporal development. The MJO signal in the zonal mean MA temperature is characterized by a particular spatial pattern in the MA, which we link to the interhemispheric coupling (IHC) mechanism, as a major outcome of this study. The ~~strongest temperature deviations are on the order of $\pm 10\,\mathrm{K}$ and are~~ signal with the largest magnitude is found in the polar ~~winter~~ MA during boreal winter ~~and the QBO~~ with temperature deviations on the order of $\pm 10\,\mathrm{K}$ when the QBO at $50\,\mathrm{hPa}$ is in its easterly phase. Other atmospheric conditions and locations also exhibit temperature signals, which are, however, weaker or noisier. We also analyze the change of the temperature ~~response pattern~~ signal while the MJO progresses from one phase to the next. We find a gradual altitude shift of parts of the IHC ~~response~~ pattern, which can be seen more or less clearly depending on the atmospheric conditions.

The ~~found~~ statistical link between the MJO and the MA temperature highlights illustratively the ~~far reaching~~ far-reaching connections across different atmospheric layers and geographical regions in the atmosphere. Additionally, it highlights close linkages of known dynamical features of the atmosphere, particularly the MJO, the IHC, the QBO, and SSWs. Because of the wide coverage of atmospheric regions and included dynamical features, the results might help to further constrain the underlying dynamical mechanisms and could be used as a benchmark for the representation of atmospheric couplings on the intraseasonal timescale in atmospheric models.

1 Introduction

The Madden-Julian oscillation (MJO), first documented by Madden and Julian (1972), is known as the dominant mode of intraseasonal variability in the tropical troposphere (Zhang, 2005). ~~The major directly observable feature is a center of anomalously strong deep convection, flanked by regions of reduced convection. This structure appears periodically over the Indian Ocean and travels eastward over the maritime continent until it disappears over the Pacific Ocean. The MJO is a~~ It is a highly variable feature of the atmosphere ~~and~~so that, e.g., its period varies strongly between about 30 and 90 days (Zhang, 2005). Its appearance influences weather patterns in many equatorial regions, e.g., the monsoons in Asia and Australia (Zhang, 2005).

~~Although the obvious convective disturbance is limited to the Indo-Pacific region, dynamical anomalies, e.g., in terms of vorticity,~~ Dynamical anomalies connected to the MJO are measured around the whole equator (e.g., Cassou, 2008). Moreover, the MJO has also influences around the whole globe and is itself influenced from extratropical regions making the MJO a component of global teleconnection patterns (Lau and Waliser, 2012, Chapter 14). ~~A prominent example in the northern hemisphere is a link between the MJO and the North Atlantic Oscillation (Cassou, 2008). Affected are different parameters of the polar climate system like the Arctic surface temperature (Yoo et al., 2012) or even the Arctic sea ice concentration (Henderson et al., 2014).~~ For a review of the observed teleconnections between the tropics and the polar regions on different time scales see, e.g., Yuan et al. (2018).

Due to the intraseasonal time scale on which the MJO acts, a deeper knowledge on the processes that control it is expected to improve the forecast skills of longer-term weather forecasts (e.g., Zhang, 2013). The understanding of the mechanisms of the teleconnections is important to improve the representation of the MJO in models but might in turn help to improve the forecasts skills also in the extratropics, e.g., in terms of the prediction of extreme weather events (Lau and Waliser, 2012, Chapter 14). ~~Mechanisms for the teleconnections with the extratropics are reviewed by, e.g., Yuan et al. (2018). Inner-tropospheric interactions are based on the excitation of Rossby waves by the strong convection, which is associated with the MJO and propagation of zonal mean zonal wind anomalies, which are triggered by the MJO.~~

~~A further~~ Garfinkel et al. (2012) proposes a special mechanism for MJO-related teleconnections~~is proposed by Garfinkel et al. (2012) for the extended boreal winter season. It also~~, which considers the propagation of Rossby waves ~~, but this time not only the horizontal poleward propagation but also the vertical propagation~~ into the stratosphere. These waves could influence the polar vortex and modulate the appearance of midwinter major sudden stratospheric warmings (SSW), so that SSWs follow certain MJO phases. It was already known that the occurrence of ~~sudden stratospheric warmings (SSW)~~ SSWs during Arctic winter can then influence the tropospheric state below ~~(e.g. Baldwin and Dunkerton, 2001). The complete chain can therefore lead to an influence of the MJO on the polar troposphere mediated by the stratosphere with a longer time scale (one to two months) than the inner-tropospheric connections.~~ (e.g., Baldwin and Dunkerton, 2001).

There is also increasing evidence that the variability of the MJO itself is partly controlled by the stratosphere. A prominent example for this is the influence of the quasi-biennial oscillation (QBO~~; see Baldwin et al. (2001) for a review of the QBO~~) during boreal winter: Yoo and Son (2016) found that the MJO amplitude tends to be larger during the QBO easterly phase and

smaller during the QBO westerly phase and several studies followed up on this (e.g., Son et al., 2017; Marshall et al., 2017; Zhang and Zhang, 2018; Densmore et al., 2019; Wang and Wang, 2021). The influence on the MJO from above is also covered by a more general recent review ~~on the stratospheric influence on the tropical troposphere~~ by Haynes et al. (2021).

Consequently, there is increasing awareness for the potential of considering troposphere-stratosphere couplings in both directions in weather prediction systems, as shown by, e.g., Domeisen et al. (2020). And at least from these examples, it becomes clear that it is of importance to consider at least the stratosphere to completely understand the functioning ~~and interactions~~ of the MJO in the climate system.

In addition to this troposphere-related motivation, there is a second major motivation to study the connection of the MJO and the middle atmosphere (MA), which arises from the interest in the variability of the MA itself. ~~One important aspect of MA research is the determination of a long-term trend in MA temperature~~ A major aim is the disentanglement of all the sources of temperature variability, like, ~~which is an important indicator of anthropogenic climate change (e.g., Randel et al., 2009; Santer et al., 2013;~~ ~~. Other aspects are,~~ e.g., ~~the understanding of the implications of solar variability on the climate system (e.g., Gray et al., 2010)~~ ~~, the influence of large~~ solar variability (e.g., Gray et al., 2010), volcanic eruptions (e.g., Timmreck, 2012), ~~and of course the monitoring of~~ anthropogenic climate change (e.g., Randel et al., 2009; Santer et al., 2013; Maycock et al., 2018; Beig et al., 2003; Beig, 20 ~~,~~ and the change in stratospheric ozone. ~~All these aspects have in common that they are connected to temporal variability of different MA parameters, with temperature being an essential one. A major difficulty is the disentanglement of all the sources of temperature variability and the unambiguous attribution to the respective causes to understand the individual processes separately.~~ In order to increase the robustness of ~~analyses and interpretations~~those analyses, also the smaller sources of temperature variability should be known and quantified.

The MJO has, to our knowledge, gotten only little attention as ~~a~~ one possible independent source of temperature variability in the MA. In addition to the already mentioned analysis by Garfinkel et al. (2012), the studies by Yang et al. (2017, 2019) are in this context of relevance for our analysis. ~~These publications cover the MJO influence on the MA temperature among other parameters for different geographical regions, seasons and atmospheric conditions.~~ They are mostly based on modeled and reanalyzed data, whereas it is our aim to provide a purely observational perspective. Sun et al. (2021) analyze the effect of the MJO on the northern mesosphere during boreal winter. They also mostly rely on modeled data but use satellite observations as support, particularly, the same observational dataset as we use in the following (Sect. 2.1). There are more studies relevant in the broader context, but either they treat the influence on temperature not as the main point (e.g., Moss et al. (2016); Tsuchiya et al. (2016); Wang et al. (2018a)~~, which focus on the MJO influence on wave activity~~) or are limited to different atmospheric regions (e.g., Yang et al. (2018); Kumari et al. (2020, 2021)~~, which discuss the MJO influence on tides in the mesosphere / lower thermosphere region). The relationships to the relevant studies are discussed in more detail below (Sect. 4).~~).

We note as an additional aspect for the motivation that the occurrence rates of individual MJO phases appear to be subject to climate change (Yoo et al., 2011). Therefore, a linkage of the MJO and the MA could represent an additional pathway of anthropogenic climate change into the MA. Conversely, the characterization of the MJO-MA relationship might also be helpful to understand climate change related changes in the teleconnection patterns mentioned above.

All the above-mentioned aspects motivate the exploration of already existing observations with respect to the influence of the MJO on the MA, particularly on the MA key parameter temperature. However, the mentioned publications on the MJO influences on the MA temperature mostly deal with modeled or reanalyzed data, which has the advantage that respective mechanisms can be more easily identified in these more comprehensive datasets. Contrarily, this publication aims at contributing a global quantification of the influence of the MJO on MA temperatures based observed data, to gain additional independent and purely observationally determined information to complement modelling efforts.

Most related studies first determine the MJO phase with the strongest response and concentrate in the following analysis mostly on this phase (e.g., Garfinkel et al., 2012; Yang et al., 2017). The temporal evolution of the atmosphere is then considered in time lags around the appearance of this phase. We ~~consider instead~~ instead consider all eight MJO phases, so that the transition of the MA temperature response from one MJO phase to the next becomes visible. Furthermore, we concentrate in this paper on the analysis of zonal mean temperatures ~~for the sake of brevity. Nevertheless, the dataset provides also a wealth of three-dimensionally resolved information, which we intend to present in a later paper.~~.

The ~~present~~ paper contains a description of the datasets and methodology in Sect. 2. The results, i.e. the zonal mean MA temperature responses to the individual MJO phases for different atmospheric conditions, are shown in Sect. 3. Section 4 contains an extensive discussion, in which the results are related to known dynamical features of the MA, before we conclude the paper in Sect. 5

2 Datasets and analysis approach

2.1 Datasets

We analyze the temperature data product measured by NASA's Microwave Limb Sounder (MLS) on the Aura satellite (Schwartz et al., 2020), version 5. A previous version of the dataset has been validated by Schwartz et al. (2008). Differences to the new version are mentioned in Livesey et al. (2020). Data screening and exclusion has been performed according to all suggestions in the MLS quality document (Livesey et al., 2020), including the screening for cloud effects based on the MLS ice water content (IWC) product. We analyze the complete reasonable vertical range from $261\,\mathrm{hPa}$ to $0.00046\,\mathrm{hPa}$ and also use the complete temporal coverage of the ongoing measurements of about 17 years at the time of the analysis (approximately August 2004 to September 2021). The data has a spatial resolution, which roughly decreases with height in a range from about $4\,\mathrm{km}$ vertical and $170\,\mathrm{km}$ horizontal resolution at $261\,\mathrm{hPa}$ to $13\,\mathrm{km}$ vertical and $316\,\mathrm{km}$ horizontal resolution at $0.00046\,\mathrm{hPa}$ (Livesey et al., 2020). The data has been analyzed on the original pressure grid. One has to keep in mind that the analysis grid is finer than the varying vertical resolution and that adjacent altitudes are not completely independent of each other. The original data follows the satellite track and has been averaged to fit onto temporally and horizontally regular grids. Particularly, for this paper we apply a zonal averaging with $10°$ resolution in the latitudinal direction.

For the characterization of the MJO, we use the OLR-based MJO Index (OMI; OLR stands for outgoing longwave radiation) introduced by Kiladis et al. (2014). We calculate the OMI values from OLR using the open source OMI calculation package (Hoffmann et al., 2021; Hoffmann, 2021), version 1.2.2. According to Hoffmann et al. (2021) a high agreement ~~between~~

with the original calculation routine, which is close to being identical, is expected. For the calculation, interpolated OLR data according to Liebmann and Smith (1996) has been used. From the two OMI index values per time step, the phase and the strength of the MJO for each day can easily be calculated following the phase diagrams in Kiladis et al. (2014) and Wheeler and Hendon (2004).

We note that the MJO is subject to a seasonal variability (e.g., Zhang, 2005). The common MJO concept with the characteristic eastward propagation applies best for boreal winter. During boreal summer, the propagation direction includes a northward component (e.g., Wang et al., 2018b) and the feature is often given a distinct name, the boreal summer intraseasonal oscillation (BSISO). This has also implications for the definition of appropriate MJO indices and partly particular BSISO indices are used for analyses with a special focus on boreal summer (e.g., Kikuchi et al., 2012). However, since our analysis is not restricted to boreal summer and Wang et al. (2018b) states that the MJO index OMI is also capable of reasonably tracking the BSISO, we apply OMI consistently for all seasons. This has the advantage of comparability of the results for different seasons. ~~Nevertheless, we might check our boreal summer results with a special BSISO index in future.~~

For the characterization of the QBO, we use monthly mean zonal wind data above Singapore at $50\,\mathrm{hPa}$ (Naujokat, 1986). We apply the ~~most simple~~ simplest discrimination approach: positive zonal wind values indicate a QBO westerly phase and negative values a QBO easterly phase.

2.2 Approach

Our analysis approach is a superposed epoch analysis (SEA) also known as composite analysis. The complete analysis chain consists, however, of several steps, which are computed for each geolocation of the previously mentioned regular spatial grid separately.

First, a temperature anomaly is computed by applying a centered boxcar running average with a window length of $90\,\mathrm{d}$ as a low-pass filter and calculating the difference between the original and the low-pass filtered time series. Afterwards the anomaly is smoothed with a 10-day running average. The latter is mainly done for reasons of comparability with other analyses and is strictly speaking disadvantageous since it introduces a statistical dependence of the previously independent individual days. Therefore, we have checked that, in practice, the results do not change significantly when the 10-day filter is not applied. The resulting anomaly time series contains due to the filtering only strongly damped variations on much longer (e.g., the seasonal cycle) and much shorter (e.g. weather fluctuations) time scales than the MJO, but still captures a broad range of frequencies in the intraseasonal time scale, relevant to the MJO.

Second, the data is selected according to the environmental conditions. We ~~take generally only days into account, during which the MJO strength was~~ only consider those days when the strength of the MJO is greater than 1. ~~This is a common choice~~ Values between 1 and 1.5 are common choices in many MJO related studies to make sure that there is actually an MJO signature ~~apparent on all considered days~~ (e.g., Hood, 2017; Garfinkel et al., 2012, 2014; Yang et al., 2017, 2019), whereas our choice of 1 includes as many days as possible. Depending on the particular experimental setups described below, the data is also selected with respect to particular seasons and with respect to the state of the QBO. Specifically, all days, which do not match the wanted setup criteria, are removed from the dataset prior to the SEA. We consider the seasons boreal winter /
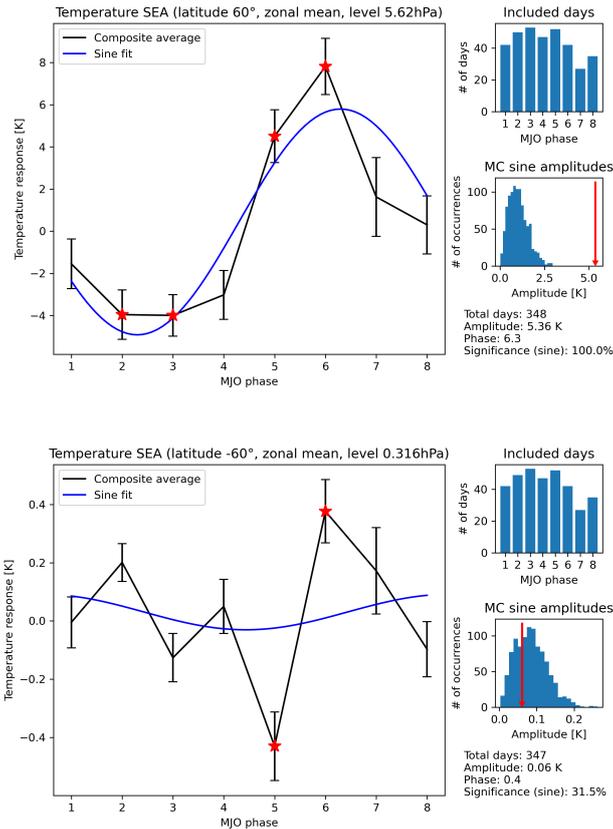
Figure 1. Examples of the temperature responses to the eight MJO phases at two geolocations for the boreal winter / QBO easterly situation. The examples have been selected for demonstration purposes to represent a particularly strong response (upper half) and a weak response (lower half). The following description applies to both cases: The main results, the average temperature anomalies for each MJO phase, are shown as the black lines in the larger panels together with the eight standard errors of the mean shown as error bars. The blue line shows the fitted sine curve. Temperature responses, which are significant according to the MCIP method (see Sect. 2.2 for details on the MC quantification) are marked with red stars. Results according to the MCS significance estimation method, which estimates the significance of a systematic variation over all eight phases, are shown in the lower smaller panels on the right, respectively: The blue bars constitute a histogram of all sine amplitudes derived based on random data, whereas the sine amplitude of the real data is shown as a red arrow. The resulting percentage of random amplitudes lower than the real one is also given in the lower right text field. The upper smaller panels on the right simply indicate how many days of the data went into each of the eight temperature anomaly average values.

austral summer (December, January and February) and boreal summer / austral winter (June, July, August). The complete set of selection criteria for a particular experiment is sometimes called "atmospheric conditions" or similar in the remainder of the manuscript.

Third, the actual SEA is carried out: the selected temperature observations are grouped by the related MJO phases of each day and then averaged, so that one temperature mean value per MJO phase is calculated, complemented by the corresponding standard errors of the mean. The basic idea is that temperature fluctuations, which are not correlated with the MJO phase propagation will average out, while fluctuations correlated with the MJO phases will add up, so that remaining epoch averaged anomalies indicate a statistical connection between the MJO phase propagation and the MA temperature. Note that we apply a small correction after this basic step: a mean over the complete data subset at the respective geolocation (i.e., independent of the MJO phase) is subtracted from all eight average values. This overall mean value is usually close to $0\,\mathrm{K}$, because the whole calculation is carried out on temperature anomalies, which are scattered around zero. However, the average of the selected subset of the data may slightly deviate from zero, which would complicate the comparison of the results for different geolocations if not corrected for. Fig. 1 shows two examples of the SEA results, which represent a strong and a weak response. The number of days that go into the individual averages depends of course strongly on the selection criteria, but also somewhat on the geolocation and the MJO phase itself. Rough numbers are about 400 days per MJO phase if only the MJO strength filtering is applied, 100 days with additionally the seasonal selection and 50 days with a combined seasonal and QBO selection.

As stated before (Sect. 1), we consider all eight phases of the MJO so that the transition of the MA temperature response from one phase to the other becomes visible. At least in an ideal case, the response could vary like sine function over the course of the eight MJO phases. Following this notion, we fit a sine function to the eight mean values as the fourth analysis step to further characterize the behavior across the MJO phases. The parameters amplitude, phase and offset can freely be adjusted by the fit, whereas the period is fixed to 8 MJO phases. The fit results can be analyzed with different foci. However, in this study only the resulting amplitudes are used for a significance estimation in the next analysis step. The two examples in Fig. 1 also show the fitted sine curves. It is seen that the strong response exhibits indeed a sine-like behavior and the amplitude roughly represents the strength of the deviations, whereas the appearance of the weak response is ~~more noisy~~noisier, which results in ~~a~~ an even weaker sine amplitude.

The fifth and final step is a significance estimation using a Monte Carlo (MC) method. For this, the analysis is basically repeated multiple times, each time with randomly modified input data. The resulting distribution of artificial results can be used to estimate how likely a particular temperature response can be the result of random fluctuations instead of physical reasons. As we have pointed out in Hoffmann and von Savigny (2019), there is a wide scope of individual decisions in the design of the MC calculations, which can influence the final significance estimation. In order to not distract the reader from the basic results, we concentrate here on only one version of the random data generation (as most other publications also do), which is well comparable to many previous publications. Particularly, we randomly redistribute the MJO index time series 1000 times, i.e. the attribution of MJO phases and strengths to the individual days of the time series is changed. The temperature data remains thereby untouched. The SEA calculation is repeated for each random data realization resulting in a distribution of possible temperature responses. Whereas we only present one kind of random data generation, we still show two different kinds of the final quantification of the significance. The first one, abbreviated as MCIP for "Monte Carlo Individual Phases" in the following, is also best comparable to previous studies, particularly if they are focused on individual MJO phases. It is simply checked for each MJO phase separately if the absolute value of the real SEA anomaly result for a particular MJO phase

195 is greater than 95 % of the absolute values of the responses based on random data. Hence, this significance estimation checks
if the derived SEA temperature anomaly is strong enough to be only very unlikely produced by random fluctuations for each
MJO phase separately. Significant average values according to this method are marked with a red star in Fig. 1. An advantage
is that this significance estimation exists separately for each MJO phase. However, this method has the disadvantage that it
may underestimate significance. E.g., if ~~a~~ we consider the result for MJO phase 1 in the upper panel of Fig. 1, the response
200 is relatively close to 0 K and consequently also likely reproduced by random data and therefore not marked as significant.
However, the development of the response over all eight MJO phases indicates that the response of phase 1 could be a part
of an overall systematic variation, albeit approximately at the zero-crossing of the variation. Therefore, we use a second
quantification approach, abbreviated as MCS for "Monte Carlo Sine" in the following, in which it is checked that the real
amplitude of the fitted sine function is greater than 95 % of the fitted amplitudes based on the random data. Hence, this
205 quantification approach evaluates the systematic behavior over all 8 phases and is therefore also based on a larger number
of samples (all days that go into the eight averages instead only those, which go into one specific average). Examples of the
distributions of sine amplitudes are also given in the lower smaller plots in Fig. 1.

We would like to point out that the overall approach aims at establishing a statistical connection between the MJO phase
evolution and the MA temperature without probing a causal or physical connection. Strictly speaking, also the direction of
210 ~~the~~ an influence is not checked. However, ~~on the one hand,~~ describing a statistical connection first helps to clearly define
the observational aspects, which the ultimately sought physical mechanism has to cover. This is the basic aim of ~~the present~~
~~manuscript. On the other hand, by considering previous publications, which overlap in particular aspects, it becomes expectable~~
~~that a physical mechanism actually exists (i.e. that we do not describe a purely statistical artifact) as we will outline in Sect. 4.~~

3 ~~Results: MJO influence on zonal mean MA temperature~~

215 ~~This study is focused on the zonal mean response of MA temperature to the MJO. Nevertheless, a quick inspection of the full~~
~~three-dimensional structure of the response exhibits also zonal structures, particularly in~~ this study. The reader should keep this
statistical nature of ~~the~~ ~~lower stratosphere. These structures partly cancel out by the zonal averaging so that the zonal mean~~
~~anomaly values shown in the following are likely lower than some of the individual local responses.~~

2.1 ~~No filtering for environmental conditions~~

220 ~~As will become obvious in the following, external conditions like the season and the QBO have a strong influence on the~~
~~strength and spatial structure of the response.Hence, analyzed data that comprises different states of these conditions might~~
~~also result in reduced responses due to interferences of the individual responses to these conditions.Therefore, we do not discuss~~
~~the unfiltered analysis here in detail. Nevertheless, we show the results for the unfiltered data (only a filtering for MJO strength~~
~~greater than 1 is applied) in the supplement (Fig. S1) and note here that the derived temperatureanomalies connected to the~~
225 ~~MJO influence are in this case in the range of ±2K~~ analysis in mind for the whole manuscript independent of the particular
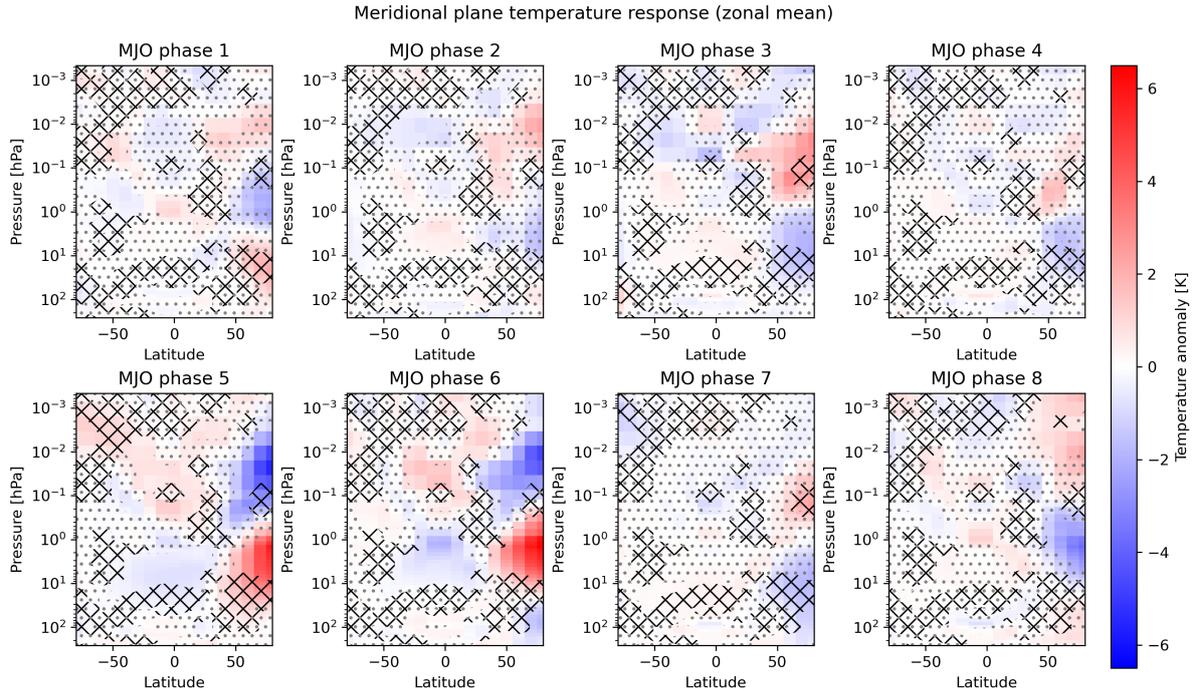
Figure 2. Meridional plane temperature responses for all eight MJO phases for the boreal winter / austral summer situation. Each panel contains the temperature anomaly response to a particular MJO phase for all geolocations in the zonal mean. All eight panels share the same color scale on the right. Insignificant values according to the MCIP method are marked with gray dots. Insignificant areas according to the MCS method are marked with black crossed lines. Note that the insignificance pattern according to the MCS method is identical for all 8 MJO phases, since the overall systematic behavior is evaluated (slight differences of the hatches between the different panels are due to numerical inaccuracies in the rendering of the image and do not indicate differences in the significance estimation results).

wording. E.g., if the verbs "influences" or "affects" are used together with the MJO effects on MA temperature, we always refer to our statistical approach.

3 Results: MJO signals in zonal mean MA temperature

3.1 Boreal winter / austral summer

230 We start with the data restricted to boreal winter, since ~~it is known that the strongest signal is likely produced by the MJO during that season.~~this season is the focus of many related studies (see Sect. 4). Fig. 2 shows the meridional plane temperature responses for each of the eight MJO phases. The strongest response is seen for the MJO phases 5 and 6 in the northern polar region, i.e., in the winter hemisphere. This response is spread vertically and divided into two zones with opposite sign visible
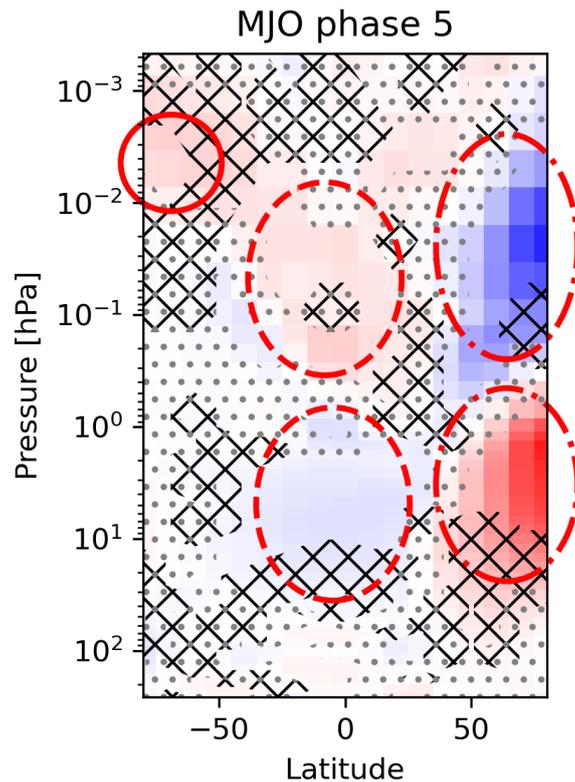
Figure 3. Repetition of the data shown for MJO phase 5 in Fig. 2, but with the ~~five-zone-response~~ five-zone-signal highlighted to guide the reader better through the written description. The two dash-dotted circles indicate the two zones of the polar winter dipole in the temperature response. The two dashed circles mark the corresponding equatorial dipole, which has a reversed sign compared to the polar dipole. The solid circle marks the fifth anomaly zone located in the summer mesosphere, which has the same sign as the upper equatorial anomaly. See Sect. 3.1 for details.

as strong red and blue areas in the figure. The departures from the mean state are as high as $\pm 6\,\mathrm{K}$ even in this zonal mean
235 picture.

A broader overall pattern in the meridional plane response can be recognized ~~more or less for each MJO phase. However, it~~ for most MJO phases. It is also clearest for MJO phase 5, so that ~~this phase serves as an example and is~~ these results are shown again with some visual guidance in Fig. 3 to support the following description: The two strong anomalies over the winter pole described before (indicated with dash-dotted circles in Fig. 3) constitute a vertical dipole with the positive anomaly
240 around $3\,\mathrm{hPa}$ and the negative anomaly around about $0.03\,\mathrm{hPa}$. This dipole is part of a remarkable global structure, which comprises three more zones of spatially coherent anomalies. The departures from the mean state for these three zones are with less than ~~roughly~~ 1 K much weaker than the polar ones, but are still mostly significant, particularly when considering the MCS significance estimation. Two of these weaker anomalies constitute another vertical dipole in similar altitudes as the first one,

but located around the equator (indicated with dashed circles in Fig. 3). This equatorial dipole has ~~, however,~~ opposite sign

245 compared to the polar dipole, so that all four zones together look like quadrupole spanning over the complete winter MA. ~~Put in other words, areas of mutually opposing responses between the stratosphere and the mesosphere as well as the equatorial and the polar winter latitudes can be identified. Whereas these four zones are roughly found in the winter hemisphere, the~~ In contrast, the fifth response zone is located in the summer polar latitudes (indicated with a solid circle in Fig. 3). It is even higher up between 0.01 hPa and 0.001 hPa and its extent is much smaller than ~~that of the first four zones~~ the quadrupole pattern lower

250 down. It shows a positive anomaly and looks like a polar summer mesosphere extension of the positive equatorial anomaly around 0.1 hPa. As we will come back to this pattern several times, we ~~will call it temporarily~~ denote these MA anomalies temporarily by "~~five-zone-response~~ five-zone-signal" for a clearer identification in the following. But we note that this pattern has already been described in the context of a dynamical feature in the MA, the interhemispheric coupling, as we will discuss in Sect. 4.1.

255 The ~~five-zone-response appears more or less intense~~ five-zone-signal appears with varying clarity for each of the MJO phases~~while it~~ , but has an opposite sign for some ~~of the~~ phases (compare, e.g., the responses for the phases 2 and 6 in Fig. 2). Of interest could therefore also be the transition of the response from one MJO phase to the next to get an idea of possible temporal systematics. For some of the phases, a gradual systematic change of the response is indeed recognizable, e.g., a downward shift of the polar winter dipole from MJO phase 2 to phase 4. Furthermore, some of the opposite MJO phases show

260 also temperature responses with an opposing sign, as expected for an ideal temperature oscillation during the course of one MJO cycle (e.g., the previously mentioned phases 2 and 6). However, the mapping of the responses of opposite phases is not perfectly symmetric. ~~E.g., the phases 5 and 6 appear to be opposed by the phases 2 and 3 instead of 1 and 2 and the responses of the opposite phases 3 and 7 show roughly no sign switch at all.~~ We will elaborate on the aspect of the phase transition ~~in the context of the QBO influence in~~ during the course of the following Sect. 3.2.

265 ~~We note that the northern winter middle atmosphere is, of course, known to be subject to strong variability in any case, which is connected to the properties of the polar vortex and particularly the appearance of SSWs. Hence, one might argue that our observation that the strongest response appears particularly in this region suggests that it is a statistical artifact, i.e. that it is caused by strong uncorrelated fluctuations, which are not sufficiently averaged out. Indeed, it cannot be totally excluded that parts of the strong uncorrelated variability would remain in the averaged data, but we discuss some arguments supporting the~~

270 ~~existence of a real signal in Sect. 4.2. Particularly, SSWs could be themselves influenced by the MJO and therefore be part of the mechanism producing the temperature signals found here.~~

3.2 Boreal winter / austral summer and state of the QBO~~easterly~~

Fig. 4 shows a similar analysis but with data selected for boreal winter and QBO easterly conditions. Overall, the responses look similar to those for boreal winter data (Fig. 2; note that the color scale has a different range). Particularly the ~~five-zone-response~~

275 five-zone-signal is recognizable for each MJO phase, although the responses for the MJO phases 1 and 8 look somewhat disturbed (which will become part of the interpretation below). The significant part of the summer mesosphere extension appears generally to be higher up at around 0.001 hPa for the boreal winter and QBO easterly situation. It is ~~obvious~~ evident
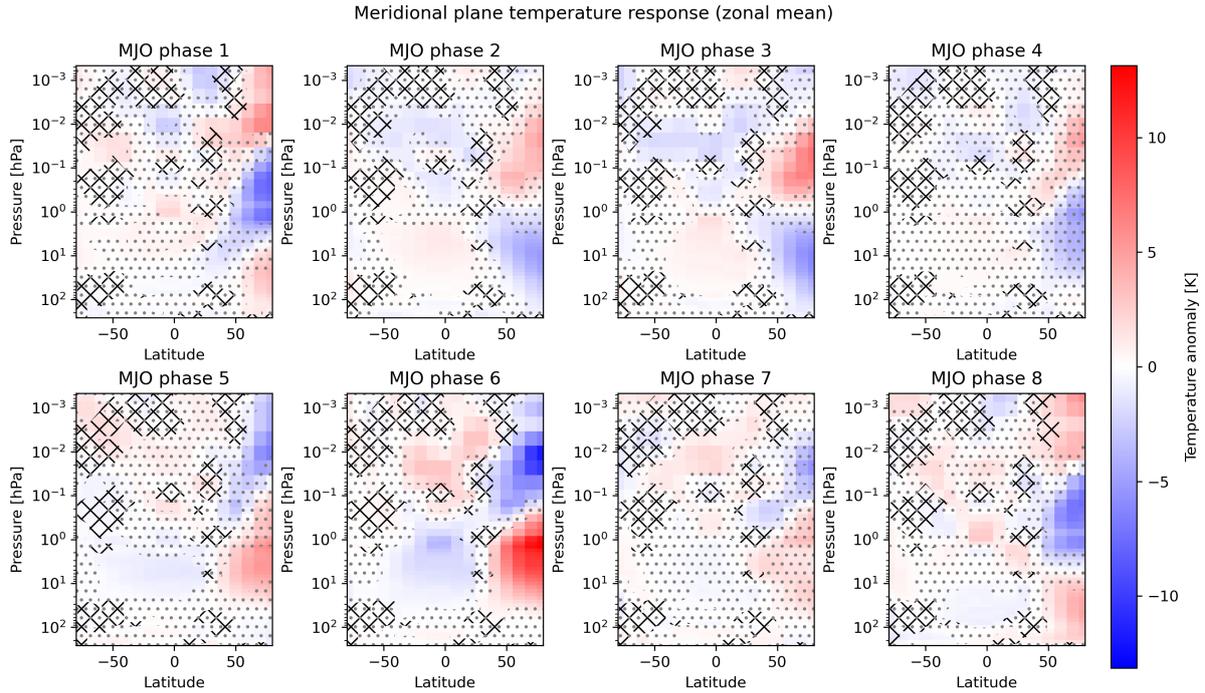
Figure 4. Similar to Fig. 2 but for the boreal winter / austral summer and QBO easterly situation. Note that the color scale is different compared to Fig. 2.

that the temperature anomalies ~~are even stronger than for boreal winter filtering alone.~~ in the boreal winter with QBO easterly conditions are of larger magnitude than those shown in Fig. 2. The strongest response is again seen in MJO phase 6, here now
280 on the order of $\pm 10\,$K.

~~It is of interest to look again at the transitions of the response patterns~~ The transition of the five-zone-signal between different MJO phases ~~, which now emerge~~ emerges now more clearly: At a simple level, ~~it is seen that roughly~~ two classes of the response pattern ~~exist, which correspond to the one or the other sign of the five-zone-response anomalies. Important~~ can be identified, corresponding to both signs of the five-zone-signal. The importance is the ordered appearance of these two classes: one class
285 is coherently observed during the first half of the MJO cycle (particularly during the phases 2 to 4 during which, e.g., the polar winter stratosphere is colder than normal), whereas ~~as~~ the other class is seen for the second half of the MJO cycle (particularly during the phases 5 to 7 during which, e.g., the polar winter stratosphere is warmer than normal). This coherent behavior ~~, with opposing MJO phases showing roughly temperature responses with also opposing signs,~~ further supports that a real systematic response to the MJO is found here. The responses to the phases 1 and 8 are somewhat more difficult to interpret since the polar
290 winter anomaly dipole is extended by a third anomaly zone higher up. However, these phases can be systematically integrated in a more detailed recognition of the response transitions between the MJO phases as detailed in the following.

Looking more closely, a gradual change of the response from one MJO phase to the next within the two classes is seen in terms of a descent of the response pattern. This is most easily seen in the second half of the MJO cycle by starting with MJO phase 5 and following the ~~negative polar winter anomaly~~ cold anomalies in the boreal polar winter with the eyes (blue area in the upper right of the MJO phase 5 panel in Fig. 4): The negative anomaly is there in the highest altitudes and then descends in the following MJO phases including phase 8. Such a behavior can also be roughly identified during the first half of the MJO cycle, when starting in MJO phase 1 with the upper positive polar winter anomaly (red area in the upper right of the MJO phase 1 panel in Fig. 4) and following its vertical position towards phase 4. Note that the summer mesosphere extension of the ~~five-zone-response~~ five-zone-signal remains at its altitude during all eight MJO phases.

Moreover, one could also combine the gradual changes within both classes to a roughly continuous descent during the course of a complete MJO cycle. This is most easily seen when starting again in phase 5, but this time with the positive stratospheric winter anomaly (red area on the right at about $5\,\mathrm{hPa}$ of the MJO phase 5 panel in Fig. 4). Although somewhat more irregular, this anomaly descends down to about $100\,\mathrm{hPa}$ in MJO phase 8. Now, the additionally appearing polar positive anomaly area in the highest altitudes during the phases 8 and 1 could be seen as replacement for the vanishing positive anomaly in the lowest altitudes. Then the descent could be continued in MJO phase 1 with the upper positive polar winter anomaly as before. Hence, the special responses of the phases 8 and 1 would realize the transition from the one class of the response to the other class.

The only pronounced discontinuity of the transition appears between the MJO phases 4 and 5, where the sign of the response is abruptly switched. Therefore, the response evolution could be interpreted in a way that it starts in phase 5, descends during the following MJO phases including 8 and 1 until the pattern looks reversed in its sign and is then abruptly reset into its original state after MJO phase 4. However, one could also ~~speculate that the MJO phases~~ argue that this abrupt transition is just a statistical artifact, since the signal in MJO phase ~~4 or 5 should also have a third polar anomaly zone, which is only by chance not very pronounced in this particular dataset. Such a third anomaly zone should this time be negative (opposed to the third zone of the phases 1 and 8), which would then indicate~~ 4 is relatively weak and insignificant. This leaves room for the speculation that a smooth backward transition ~~and, therefore, close the cycle of the MA temperature response during one MJO cycle. Although we have here no convincing indication for the existence of such a third zone, the speculation is motivated~~ could actually be realized in reality and become visible with a longer dataset. This speculation is further underpinned by the following discussion of the austral winter situation (Sect. 3.3).

~~We~~ Note that we have used the boreal winter and QBO easterly situation to describe the two response pattern classes and the gradual transitions, since both are most clearly visible for this case. But at least the two response classes and in outlines also parts of the gradual transition can also be seen for other atmospheric conditions.

We ~~would like to emphasize once more the statistical nature of the analysis. Particularly, we do not say that a particular MJO phase is the causal reason for the MA temperature pattern, which we obtain for that phase. Since propagation speeds have to be considered in a physical mechanism, it seems more likely that a pattern seen for one MJO phase has been triggered by previous MJO phases. This is, however, not problematic for our interpretation, since we only aim at a statistical description of the MA temperature anomaly at given states of the MJO independent of the physical mechanism. This description can still be used to constrain potential physical mechanisms, since a suitable mechanism should be able to reproduce also the statistical results~~

~~presented here. We expect that particularly the coherent transitions of the responses between the MJO phases will be a helpful~~ ~~constraint for the temporal behavior of potential mechanisms.~~

3.3 ~~Boreal winter and QBO westerly~~

~~Similar to Fig. 4 but for the boreal winter / austral summer and QBO westerly situation. Note that the color scale is different~~ ~~compared to Fig. 4. We have also~~ have also checked the MA temperature response for the boreal winter and QBO westerly situation (Fig. 5) and find that it is much less clear than in the previously described boreal winter and QBO easterly case~~(Sect.~~ ~~3.2)..~~. This meets the expectations as will be further discussed in Sect. 4.5. Nevertheless, the ~~five-zone-response~~ five-zone-signal is also recognizable for some of the MJO phases~~(Fig. 5). Also other features like the third polar anomaly zone above the polar~~ ~~dipole are visible again (MJO phase~~, particularly the phases 5 ~~in Fig. 5). The strongest response appears in MJO phase 5 and is~~ ~~on the order of ±6 K, which is the same order of magnitude as for the boreal winter situation without QBO filtering. Therefore,~~ ~~the MJO influence on MA temperature has not totally vanished and has probably also to be considered under QBO westerly~~ ~~conditions. The~~ and 7. Hence, the MJO signals in MA temperature might not have totally vanished, so that the corresponding structure might become clearer in the future, when longer observational records are available.

~~Still, we would like to mention that the responses to the individual MJO phases have roughly the opposite sign compared~~ ~~to the respective MJO phase for QBO easterly filtering, although shifts in the altitudes of the response features make a 1-to-1~~ ~~attribution difficult (compare, e.g., phases 2 and 7 in Fig. 4 and Fig. 5). Furthermore, the MJO phase 5 appears to have the same~~ ~~special role as phases 1 and 8 for QBO easterly filtering. Hence, the appearance of this feature is also shifted by about half of~~ ~~an MJO cycle.~~

3.3 Austral winter / boreal summer

The analysis of the data restricted to austral winter (Fig. 6) shows generally that the previously described boreal winter ~~responses~~ signals can also be detected in the southern hemisphere, although they are weaker and ~~more patchy~~patchier. The strongest anomalies are again found in the polar winter regions, but have with $\pm 3\,\mathrm{K}$ only half of the magnitude compared to the boreal winter data, which has not been filtered for the QBO (Fig. 2). The polar winter ~~response~~ signal shows generally again the pattern of a vertical dipole, while individual exceptions with a third zone exist also here, e.g., for the MJO phase 5. The equatorial vertical dipole is partly ~~somewhat~~ more difficult to identify but is still clearly visible for many MJO phases, at least for the phases 3, 4, 6, 7, and 8. Also the summer mesosphere extension, this time in the northern hemisphere of course, can be identified in the ~~response~~ signal of most MJO phases, e.g., for MJO phase 6. However, the summer mesosphere ~~response~~ signal is more complex for some of the MJO phases: It has a dipole structure itself (e.g., MJO phases 3 and 7). It is expected from the previous results that the summer mesospheric anomaly has the same sign as the upper part of the equatorial dipole, which is actually seen also for these phases. But in addition, we find another anomaly zone above, which has the opposite sign, forming a summer mesospheric dipole. It is remarkable that this dipole also reverses the sign for the opposing MJO phases 3 and 7, which indicates a real systematic behavior.
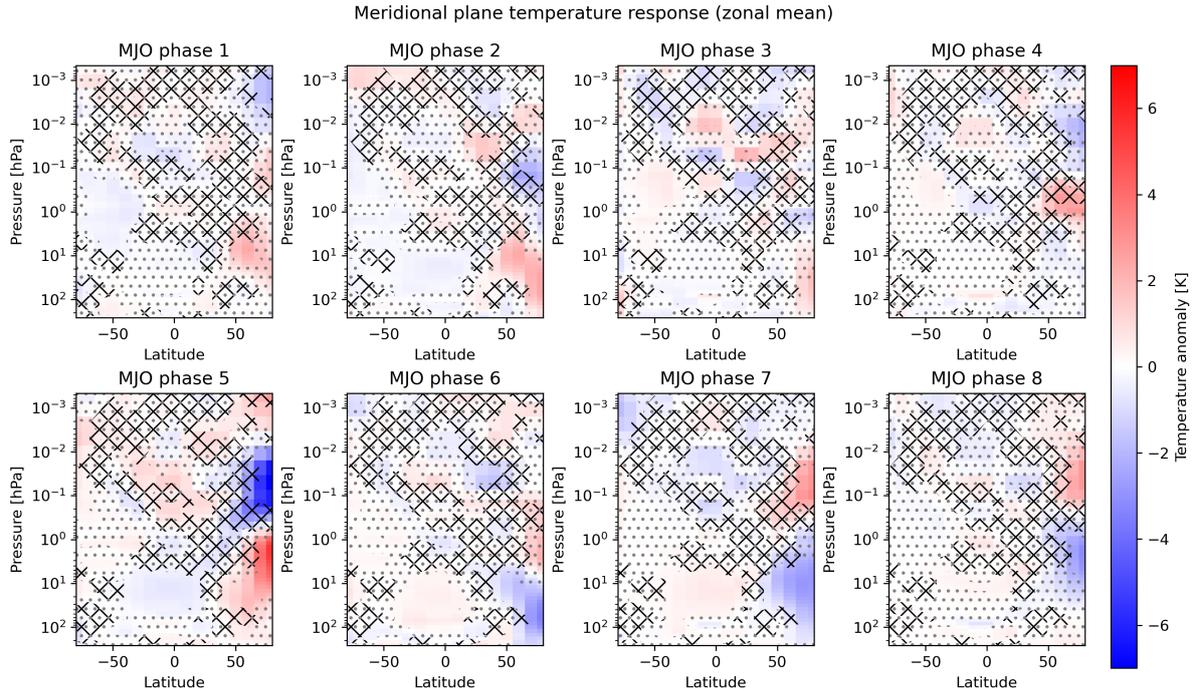
Figure 5. Similar to Fig. 4 but for the boreal winter / austral summer and QBO westerly situation. Note that the color scale is different compared to Fig. 4.

The two significance estimation approaches provide quite different results: the MCIP method shows less and smaller significant areas, which is connected to the generally weaker response. The MCS suggests instead a significant systematic response over all eight phases in almost all places of the meridional plane. Hence, although the responses are weak in terms of the individual temperature anomalies, they appear to be clearly systematically correlated with the eight MJO phases. This might be connected to the fact that this season is dynamically less disturbed so that less interfering disturbances mask the pure MJO signal.

We note that it is not necessarily expected that the austral winter response is recognizable as a counterpart of the boreal winter response and its existence appears noteworthy on its own. This is also because the austral winter hemisphere is usually dynamically much more quiescent than the boreal winter hemisphere. In particular, SSWs are very rare events in the southern hemisphere and only two such warmings have been observed since routine observations started some decades ago, namely in the austral winters of 2002 and 2019 (e.g., Jucker et al., 2021; Allen et al., 2003; von Savigny et al., 2005). While the first one is not included in the MLS period anyway, we have repeated our analysis with the MLS dataset restricted to the period before the end of 2018, so that also the second warming is not included (Fig. S2 in the supplement). It turns out that the pattern of the temperature ~~response~~ signal to the MJO phases remains basically unchanged when this warming is excluded. In contrast to
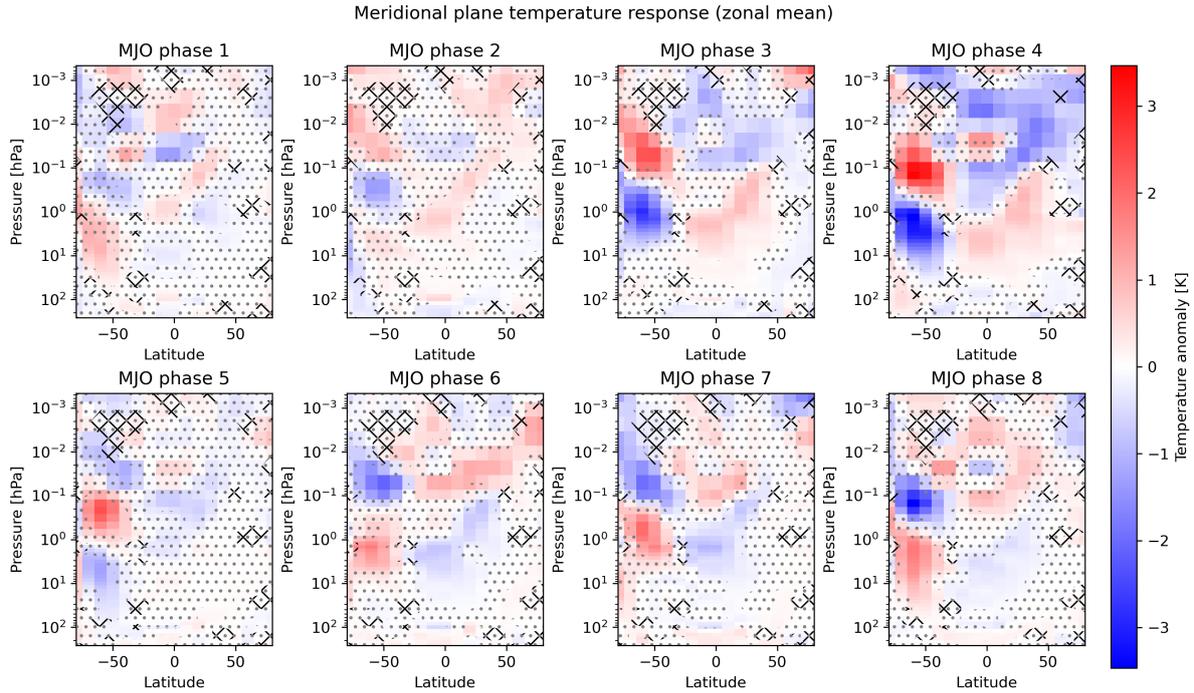
Figure 6. Similar to Fig. 2 but for the austral winter / boreal summer situation. Note that the color scale is different compared to Fig. 2.

the expectations, the strongest anomalies are even a bit stronger without 2019. This shows that the appearance of SSWs is not a precondition for the MJO-induced temperature response pattern. A fact that was unclear from analyzing the boreal winter response alone~~as discussed before (Sect. 3.1).~~ . However, due to the different magnitudes of the responses, the results still indicate that the dynamical disturbances of the boreal winter hemisphere are important for an amplification of the MJO signal.

When comparing the boreal and austral winter ~~five-zone-response~~ five-zone-signal (Fig. 2 and Fig. 6), it becomes evident that the sign of the response is identical for most individual MJO phases. This is particularly true, when comparing the austral winter response to the boreal winter and QBO easterly situation (Fig. 4 and Fig. 6), which shows a higher level of structure as discussed before. Hence, the phasing of the ~~response~~ signal with respect to the MJO trigger appears to be generally similar for both hemispheres~~(whereas it was unclear if it is maybe changed by the QBO westerly phase during boreal winter, as discussed in Sect. ??)~~ .

Also the phase transition shows similarities with the boreal winter (and QBO easterly) situation: Again~~the two classes (~~, the two different signs of the pattern ~~)~~ are seen and can again be attributed to the first and the second half of the MJO cycle, respectively. Overall, one ~~might in outlines also see here~~ can also identify the gradual descent of the pattern from one MJO phase to the next: Again, one can start with MJO phase 5 and track the upper negative polar anomaly (blue region at 0.01 hPa
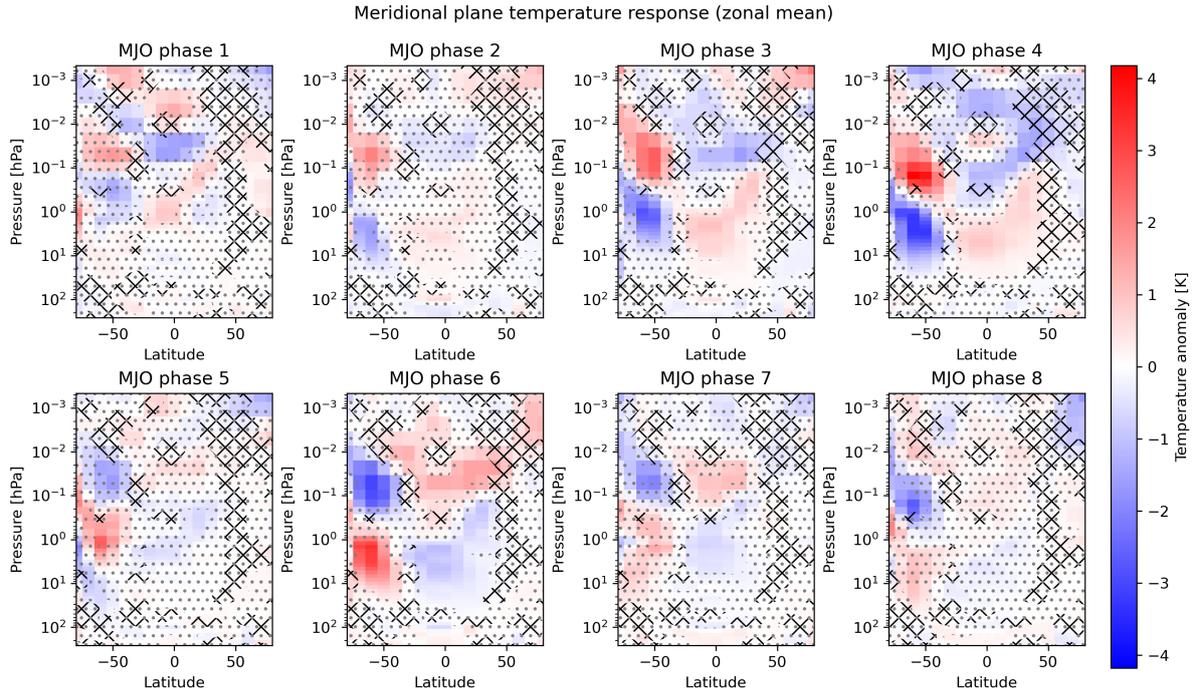
Figure 7. Similar to Fig. 6 but for the austral winter / boreal summer and QBO easterly situation. Note that the color scale is different compared to Fig. 6.

on the left of the MJO phase 5 panel in Fig. 6). It descends down to about 0.1 hPa in phase 8 and then further across phase 1 down to 5 hPa in phase 4. Note that one could also start in MJO phase 2 with tracking the upper positive polar anomaly.

But in contrast to the boreal winter / QBO easterly situation (Fig. 4), the reset of the pattern between the MJO phases 4 390 and 5 does not appear to be so abrupt Interestingly, there is no clear indication for an abrupt backward transition. Instead, a third anomaly zone (negative) appears here in the responses of the phases 4 and 5, which again suggests the interpretation as a smooth backward transition , because the lower vanishing negative anomaly can be seen as being replaced by the higher one (compare the respective similarly to the discussion of the phases 1 and 8 in Sect. 3.2). Considering that the third anomaly zone this third (positive) of anomaly zone in phase 8 , which was already discussed for the boreal winter / QBO easterly case, also 395 appears at least to some extent for also in the austral winter, one could suspect that the cycle of the temperature responses during the course of the MJO is actually closed without an in this case without any abrupt backward transition. This underpins the speculation that the alleged abrupt backward transition seen in the boreal winter / QBO easterly situation (Sect. 3.2) is actually a statistical artifact.
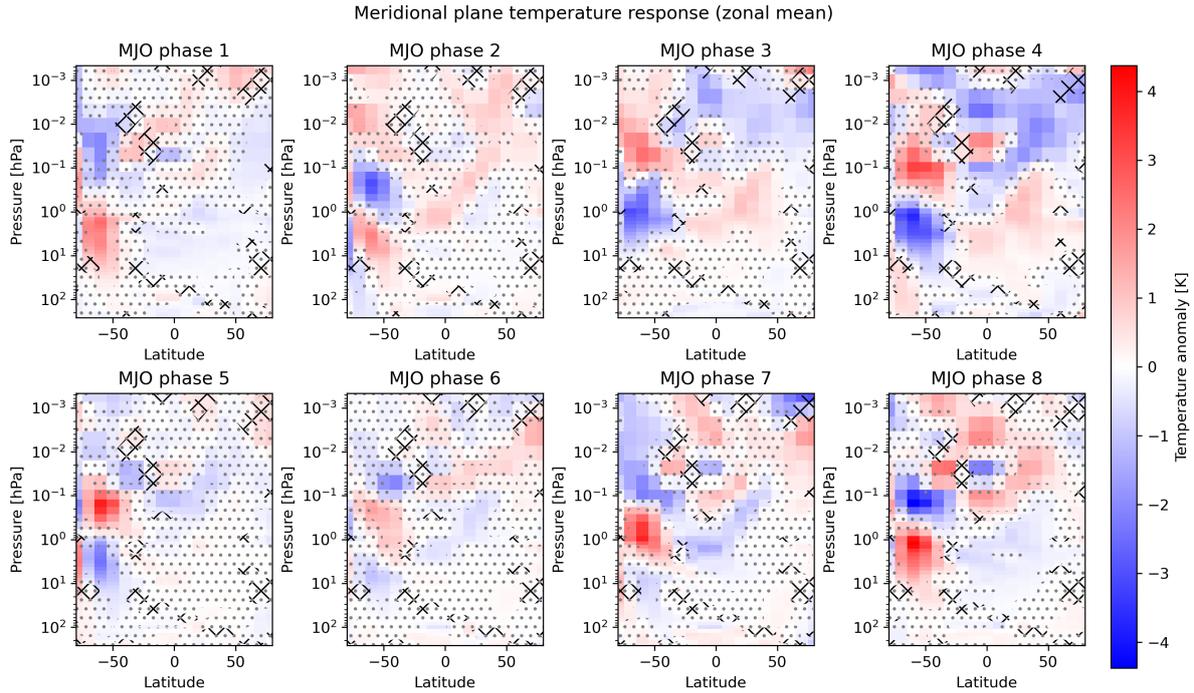
Figure 8. Similar to Fig. 6 but for the austral winter / boreal summer and QBO westerly situation. Note that the color scale is different compared to Fig. 6.

3.4 Austral winter / boreal summer and state of the QBO

400 We have also checked the QBO influence for the austral winter situation and find that the QBO has not such a big impact during this season in contrast to boreal winter situation described before. The results are shown in Fig. 7 for QBO easterly and Fig. 8 for QBO westerly. Although some differences between the MA temperature responses for QBO easterly and westerly are seen, they do not have a clear systematical structure so that these differences could also be random effects due to the different sampling periods. The only noteworthy difference is that the austral winter / QBO easterly case (Fig. 7) does not show a clear

405 descent of the pattern (nevertheless, the two classes/signs of the pattern corresponding to the first and second half of the MJO cycle are still clearly visible), whereas this descent can be seen in outlines in the austral winter / QBO westerly case (Fig. 8).

3.5 No filtering for environmental conditions

It became obvious in the previous description that external conditions like the season and the QBO have a strong influence on the strength and spatial structure of the signal. Hence, analyzed data that comprises different states of these conditions can

410 result in reduced signals due to interferences of the individual signals for different conditions. Therefore, we do not discuss the

unfiltered analysis here in detail. Nevertheless, we show the results for the unfiltered data (only a filtering for MJO strength greater than 1 is applied) in the supplement (Fig. S1) and note here that the derived temperature anomalies connected to the MJO signals are in this case in the range of $\pm 2\,\mathrm{K}$.

4 Discussion and relation of the results to previous research

415 ~~We have carved out a characteristic spatial pattern of the MA temperature response to the MJO in the meridional plane, the five-zone-response as we temporarily called it. It was~~ It is a major aim of the present ~~manuscript to communicate this broad overarching picture and particularly to include~~ paper to communicate the finding of the five-zone-signal in MA temperature in connection with the MJO as a broad overarching signal. To cover the broad picture, we included the complete meridional plane, all MJO phases, different seasons, etc. To stay focused, the study has intentionally a purely statistical character ~~and~~ so

420 that it does not determine causalities or physical mechanisms. ~~Another characteristic of the present study is that~~ Furthermore, it is mostly based on purely observational data.

There are a number of previous studies in this area of research with partly overlapping aspects. These studies are typically less broad in the above sense, but cover instead also the physical explanation approaches of the found patterns.

This section aims at briefly relating our results to the previous publications to use synergies in ~~both directions: The broader~~

425 ~~picture put up here may help to integrate and interrelate the more focused studies, whereas the more detailed considerations of the previous studies support the physical plausibility of the present statistical results and provide approaches to explanations~~ terms of two aspects: Firstly, to provide a broader picture that integrates and interrelates the current and previous studies. And secondly, to put forward some possible physical explanation in terms of the responsible mechanisms for the statistical results presented before.

4.1 Similarity with interhemispheric coupling (IHC)

430

The ~~five-zone-response~~ five-zone-signal looks qualitatively similar to the temperature pattern of a known dynamical feature of the MA, the interhemispheric coupling (IHC). IHC was first described by Becker et al. (2004) and is basically a chain of dynamical disturbances, which starts with a deviation of the planetary wave (PW) drag in the winter stratosphere~~and~~. By additionally also modifying the MA gravity wave propagation, the disturbance then spreads across the winter MA towards

435 the summer mesopause region. These dynamical disturbances cause also ~~temperatures~~ temperature anomalies with a spatial structure that is generally comparable to the one found here. A mechanism for the IHC was already proposed in the first publications (Becker et al., 2004; Becker and Schmitz, 2003; Becker and Fritts, 2006) using model experiments and then detailed by Körnich and Becker (2010). Some ~~details~~ aspects are still subject of the scientific discussion and refinement as, e.g., in Yasui et al. (2021).

440 After its discovery, the existence of IHC was further supported by satellite observations of, e.g., noctilucent clouds (Karlsson et al., 2007, 2009b) and simulations (Karlsson et al., 2009a). These simulations can be used for a quick quantitative comparison of the spatial structure with our results. This comparison reveals that the pattern fits indeed also well in terms of the pressure

levels of the strongest deviations (compare, e.g., Fig. 6 for time lag 15 d in Karlsson et al. (2009a) with our Fig. 2 for MJO phase 5, which are the periods of the strongest responses in both studies). We see, however, a much stronger magnitude of the
445 effect with about $\pm 6\,\mathrm{K}$ for northern winter filtering and $\pm 10\,\mathrm{K}$ for the northern winter / QBO easterly filtering instead of $\pm 3\,\mathrm{K}$ in Karlsson et al. (2009a).

Karlsson et al. (2009a) have further pointed out that the IHC temperature pattern can develop with both signs depending on the sign of the initial planetary wave drag disturbance. This fits to the two classes of response, which we have seen for the first and the second part of the MJO cycle, respectively. The first half fits ~~roughly~~ generally to the "weaker wave drag scenario" in
450 Karlsson et al. (2009a), whereas the second half fits to the "stronger wave drag scenario".

As an interim conclusion, we state, that the ~~five-zone-response~~ five-zone-signal is probably identical to the already known IHC temperature pattern. Hence, the MA part of the formation mechanism of the ~~five-zone-response~~ five-zone-signal is probably the known IHC mechanism.

One of the new aspects of the present study is that the emergence of the IHC pattern has now been linked statistically to the
455 MJO phase evolution~~, which~~. This leads to the ~~strong expectation~~ assumption that the MJO can indeed act as a trigger for IHC, i.e. that it can physically cause the initial PW drag deviation ~~and with that trigger the IHC~~ in both directions. ~~So far~~Previously, the IHC has been studied mainly in the context of SSW events. The MJO as a trigger is different from SSWs in such a way that, firstly, the MJO evolves continuously, periodically and relatively smoothly ~~in contrast~~ compared to the event-like SSWs. Secondly, the MJO repeats itself on the shorter intraseasonal timescale. Hence, a connected new aspect of this study is the
460 indication that the MA temperature adapts ~~in large parts of the meridional plane continuously to the PW drag~~ well up into the mesosphere continuously to tropospheric dynamical forcing changes on the MJO time scale via the IHC mechanism. A new question for the research on the IHC emerges from our observation that the pattern appears to descend during the course of the MJO. To our knowledge, an altitude-time dependence of the IHC temperature pattern has not been explicitly described or explained in the literature so far.

465 ~~We find~~ To further support that our findings are closely connected to the IHC, we list some more aspects being broadly consistent ~~with the IHC literature after quick ad hoc checks, which we mention~~ IHC publications in the following~~: First, also Yasui et al. (2021) show the SSW-triggered IHC temperature pattern (particularly their~~. The first aspect is that we see a difference of the temperature signals between the two polar regions: Whereas the polar anomaly dipole is directly located above the northern polar region during boreal winter (Fig. ~~5), which can be compared to our MJO-triggered~~ 2), it is shifted
470 somewhat more towards the equator for the austral winter situation (Fig. 6). Without going into the details of the analysis by Karlsson et al. (2007), a similar feature is seen in their results: One important indicator for the IHC is the blue area in the northern polar area in the top panel of their Fig. 2. The top panel resembles our boreal winter situation and it is seen that the blue area is directly located above the winter pole. When considering the austral summer situation (their middle panel), the blue area is not located directly above the pole but instead shifted northwards to about -50° latitude, which is basically
475 consistent with our results. ~~They use a log-pressure coordinate, which complicates the direct quantitative comparison of the vertical structure, but ad hoc attributions of the coordinates indicate that the altitudes of at least the stronger polar dipole fit quite well to our results.Note that also a descent of the pattern is implicitly shown in their data, but here related to real physical~~

time instead to MJO phases like in our analysis. A rough conversion of time lags to MJO phases indicates, however, also an overall similarity. We note that the strongest temperature anomalies found by Yasui et al. (2021) for the SSW trigger are with ±30 K much stronger than the magnitudes found here for the MJO trigger. Second, Yasui et al. (2021) The second aspect is that also Yasui et al. (2021) have not only considered a vertical dipole as the temperature response above the winter pole, but consider also see a third anomaly zone above the mesopause, which has the same sign as the stratospheric anomaly. We have also repeatedly seen this in the responses of individual MJO phases, e.g., phase 8 for the boreal winter and QBO easterly situation (Fig. 4). Third, The third aspect is that Yasui et al. (2021) partly show the summer mesospheric response of the IHC being itself a vertical dipole with a positive and a negative anomaly instead of only one zone for certain time lags. We have seen such a feature for the austral winter situation (Fig. 6). Fourth, another subtle but noteworthy detail appears when comparing our seasonally resolved results to Fig. 2 of Karlsson et al. (2007) although the quantities shown are not directly comparable: Without going into the details of their analysis, one important indicator for the IHC is the blue area in the northern polar area in the top panel of their figure. The top panel resembles our boreal winter situation and it is seen that the blue area is directly located above the winter pole. When considering the austral summer situation (their middle panel), the blue area is not located directly above the pole but instead shifted northwards to about -50° latitude. We see a similar difference when comparing the polar temperature responses of our analysis. Whereas the polar response dipole is directly located above the northern polar region during boreal winter (Fig. 2), it is shifted somewhat more towards the equator for the austral winter situation (Fig. 6).

4.2 The interconnection of IHC, SSWs and the MJO

With the present findings, a statistical triangular relation between IHC, SSW and the MJO becomes obvious: First, the IHC pattern is inherently connected to SSWs, since SSWs may produce or amplify the polar winter part of the IHC temperature pattern. Second, the occurrence of SSWs has been linked to the evolution of the MJO phases by Garfinkel et al. (2012). As a new aspect, we have now introduced the third side of the triangle, as we have statistically linked the IHC directly to the MJO. Overall, it should be expected that the connections between all the three features should be mutually consistent, which is briefly discussed in the following.

But first of all, we would like to make an aside on SSWs being a potential disturbing factor for our analysis: The SEA method is designed to average out all variability that is not correlated with the MJO phase evolution, but the success of this elimination can be reduced by unrelated variability with comparatively large magnitudes. We find the strongest responses to the MJO in the northern hemisphere winter, i.e., exactly where SSWs produce their strong variability. Hence, the objection might be raised that this strong polar winter variability is actually uncorrelated with the MJO and not sufficiently eliminated, so that the method produces false responses. While we can indeed not totally exclude that uncorrelated variability still influences the results, we have several indications that the strong polar signal is overall truly correlated with the MJO phases.: The first one is the fact that the occurrence of SSWs has been found to be itself correlated to the MJO as mentioned before and as further discussed below. Hence, the results presented here could also be interpreted as supportive for this idea instead of being an artifact. Second, we have found a similar pattern also for the southern hemisphere polar winter, which is dynamically much more quiescent and periods without SSWs can be analyzed (Sect. 3.3). Third, one could consider repeating the analysis also

for boreal winters only without SSW periods. We have quickly checked this approach, which indicated that the signature is still clearly visible. However, the number of days that go into the analysis is quite low when applying this additional filter so that the interpretation needs particular care and has not been included here.

515 We have mentioned above (Sect. 3.2 and others) that the MA temperature responses can be roughly divided into two classes with opposite sign. The responses, which roughly belong to the second half of the MJO cycle (phases 5 to 8) show a warm polar winter stratosphere and can therefore be related to the SSW case. Garfinkel et al. (2012) find MJO phase 7 as the dominating phase directly preceding SSWs (time lag of 1 to 12 days), so that the phasing is broadly consistent with our results. However, from our analyses, one would have concluded that MJO phases 5 and 6 show the strongest SSW-like responses (compare

520 Figs. 2 and 4), which might look like a discrepancy. However, the pattern in our analysis descents from phase 5 to phase 8 at least for the boreal winter / QBO easterly case, so that we see a continuous evolution of the pattern. Garfinkel et al. (2012) use instead a sharp SSW detection criterion, which is based on the atmospheric state at $10\,\mathrm{hPa}$. This is at the lower bound of the polar positive temperature anomaly found here for MJO phases 5 and 6, but more central in the positive anomaly for phase 7. Hence, what we already identify as ~~a~~ an SSW-like pattern in phases 5 and 6 might, with regard to the exact altitudes, be a

525 precursor of the SSW-like pattern considered by Garfinkel et al. (2012), which is then only reached in phase 7. This would also be roughly consistent with the result of Garfinkel et al. (2012) that MJO phase 6 is a precursor for SSWs with a longer time lag of 13 to 24 days. We note that the comparison is only a rough qualitative cross check since the analyses differ in their setups and are always complicated by the inherent large variability.

We note as a byproduct of the discussion that the descent of the IHC pattern, which has been shown in the present analysis,
530 might be relevant also for other comparisons and considerations in this area of research similar to the example above.

Overall, we consider the general consistency with Garfinkel et al. (2012) as important support for the hypothesis that the statistical relationship between the MJO and the IHC brought up in this study is a real effect and not a statistical artifact.

4.3 MJO-IHC linkage: potential coupling by planetary wave forcing

The joint reason of SSW and IHC occurrences is known to be a deviation in the PW forcing of the winter stratosphere. The
535 sign of IHC coupling pattern depends on the sign of the PW drag deviation, called strong or weak planetary wave forcing, respectively.

Our findings now ~~relate the MJO to~~ indicate a relation of the MJO and such PW drag deviations relevant to IHC: Although not proven by our statistical approach, the MJO appears to act as a source of the initial PW disturbances, which can weaken ~~and strengthen the relevant PW activity in the winter stratosphere. More precisely, the first half of the MJO cycle (~~(MJO phases
540 1 to 4) ~~tends to weaken the planetary wave activity, whereas the second half (~~and strengthen (MJO phases 5 to 8) ~~tends to strengthen it~~the relevant PW activity in the winter stratosphere.

It is therefore of interest to consider the study by Wang et al. (2018a), which explores the effect of MJO phase occurrences on wave activity in the northern hemisphere winter stratosphere~~, i. e. in the region where the IHC mechanism needs the initial PW drag deviation.~~. Wang et al. (2018a) find that a higher occurrence frequency of MJO phase 4 is in line with weaker wave
545 activity. This is roughly consistent with our findings in the sense that MJO phase 4 belongs to the first half of the MJO cycle~~,~~

for which we also find the weak PW drag case. Furthermore, Wang et al. (2018a) find higher wave activity for MJO phase 7, which is also roughly consistent with our findings, since phase 7 belongs to the second half of the MJO cycle.

The reason for the PW drag modulation is according to Wang et al. (2018a) that MJO wave activity is in antiphase with the climatologically apparent waves in the respective region for MJO phase 4 and in phase for MJO phase 7. Hence, a mechanism
550 for the relationship between the tropospheric MJO and the MA IHC pattern found in our study should probably consider such PW wave interferences as a link.

However, our results also raise new questions in this context: Wang et al. (2018a) state that all other MJO phases should not have a strong influence on the extratropical stratosphere, because there is no clear in-phase or antiphase relationship of the MJO related waves and the climatological waves. We find instead a response throughout the middle atmosphere for roughly
555 all MJO phases. This could be consistent as long as the MA responses to all other MJO phases are considered as time-lagged results of the forcings of only the MJO phases 4 and 7. This is indeed not excluded by our results, instead the nature of the responses and the gradual transitions between them is an open question. However, it is then dubious surprising that the main forcing occurs towards the end of those consecutive MJO phases, which show the appropriate sign of the response (phases 1 to 4 and 5 to 8, respectively). Hence, the explanation of Wang et al. (2018a) for all phases except 4 and 7 seems not to be in line
560 with our findings. This could mean that the mechanism, which explains our results, is more complex. But it appears also to be appropriate to question if Wang et al. (2018a) really describe the full relationship of MJO and wave activity.

4.4 Comparison with previous studies covering the relationship of the MJO and MA temperature

There are some studies already dealing with the MJO-MA temperature relationship for particular MJO phases independent of IHC, which can be compared to our results. While the present study does not go as far into possible explanations of the
565 relationship as some of these studies, it adds the overarching picture of the interhemispheric coupling to this topic, which could help to combine the previous findings. Simultaneously, the previous results can further support the statistical findings of the present analysis.

We note, however, that strict comparisons are difficult, not only because of the partly high variability of MA temperature, different analysis setups and different datasets, but also because many studies analyze the state of the MA as a function of
570 relatively long time lags after only selected MJO phases. Our analysis works without time lags and considers instead all eight MJO phases to uncover the gradual changes of the responses between the individual MJO phases. This means that comparisons have ad hoc to assign the MJO phase evolution to specific time lags by using rough mean MJO periods. Hence, the reader should have in mind that the comparisons have a rough and partly comparisons have mostly a qualitative character.

The order of magnitude of the MJO-related temperature anomaly shown in Sun et al. (2021) is with $\pm 5\,\mathrm{K}$ comparable to our
575 analysis, as well as the fact that the strongest anomalies are observed, when the polar stratosphere shows the warm anomaly. The agreement of the orders of magnitude is particularly remarkable, since the periods of strongest variability are missing due to the exclusion of SSWs in Sun et al. (2021). Also the order of magnitude of the temperature response reported Yang et al. (2019) is comparable to our results of the boreal winter situation without QBO filtering (Fig. 2), i.e., in the situation for which the analysis setups are closest to each other.

580   The northern winter polar vertical dipole of the ~~five-zone-response~~ five-zone-signal is, e.g., confirmed by Sun et al. (2021, Fig. 2). They also show the temporal switch of the dipole's sign, here between time lag $25\,\mathrm{d}$ and $30\,\mathrm{d}$ after MJO phase 4. A consistent sign change of the temperature anomaly is also found in Yang et al. (2019, Fig. 1(a)) for a time lag of $0\,\mathrm{d}$: It is seen that the stratospheric response is negative for MJO phases 2 and 3 and positive for the phases 5 and 6, as in our study.

With respect to the timing, Sun et al. (2021) report a cooling of the northern hemisphere mesosphere 35 days after MJO
585   phase 4. Yang et al. (2019) report a corresponding stratospheric warming after MJO phase 4 with a time lag of $30\,\mathrm{d}$. Although both might still fit to the appearance of this pattern in the second half of the MJO cycle in our data, we would have expected it earlier in terms of time lags after phase 4.

The results for the austral winter can be compared to Yang et al. (2017, Fig. 2 (A) and (B)). They find cold anomalies at $10\,\mathrm{hPa}$ and a time lag of $0\,\mathrm{d}$ roughly for the MJO phases 1 to 3 and warm anomalies for the phases 5 to 7. We see the
590   corresponding responses slightly shifted to the MJO phases 2 to 4 and 6 to 8, respectively, and also somewhat different in altitude, but a rough consistency can be stated. A comparison of the complete meridional plane response for MJO phase 5, which is included in Yang et al. (2017, Fig. 4), also reveals a general consistency with our results. Particularly, the results for the time lag of $10\,\mathrm{d}$ compare well to our MJO phase 6 response. Also, our magnitude of the anomalies fits roughly to the results of Yang et al. (2017).

595   ~~We note that although the study by Yoo et al. (2012) is actually focused on an inner-tropospheric MJO teleconnection, the lowest altitude levels of our analysis can still be compared to their highest levels. Without going into details, the tropospheric northern meridional plane response in Yoo et al. (2012, Fig. 6) at different time lags after MJO phase 1 and 5 resembles roughly the evolution with the MJO phases found here. Therefore, the responses at the lower altitude levels in our study are probably more a result of the tropospheric processes analyzed by Yoo et al. (2012) rather than a result of stratospheric processes~~
600   ~~discussed here so that they do not have to be explained within the dynamical framework of IHC. Furthermore, Yoo et al. (2012) report on stronger poleward Rossby wave propagation in connection with MJO phase 5 and weaker poleward wave propagation in connection with phase 1. Although this strictly applies only for the troposphere, we note that this attribution is roughly consistent with our discussion of the weak and strong wave driving IHC pattern (Sect. 4.1) and should therefore be considered when working on the questions raised in Sect. 4.3.~~

605   ## 4.5   Influence of the QBO on the MA temperature response to the MJO

For the influence of the QBO on the MJO-MA connection (e.g., Sect. 3.2), at least two possible types of interference have to be considered: The influence of the QBO on the MJO itself as well as the inner-stratospheric influence of the QBO on the polar stratospheric dynamics.

4.5.1   Influence of the QBO on the MJO

610   The influence of the QBO on the MJO is currently an active field of research and still debated (e.g., Yoo and Son, 2016; Zhang and Zhang, 2018; Wang and Wang, 2021). Overall, there appears to be a strengthening of MJO effects for the QBO easterly

phase during boreal winter, which fits qualitatively very well to our findings. Note that, combined with our results, this would be a net effect of the tropical lower stratosphere on the complete MA conveyed by the troposphere, where the MJO is active.

Regarding the seasonal differences, the QBO influence on the MJO has mainly been reported for boreal winter (e.g., Yoo and Son, 2016; Son et al., 2017). However, using two more sophisticated analysis approaches (QBO determination and BSISO index), Densmore et al. (2019) claim that there is also an QBO-MJO relationship during boreal summer, which is reversed compared to boreal winter. Our examination of the QBO influence on the MJO-MA connection during boreal summer (Sect. 3.4 and Figs. 7 and 8) showed no clear indication for a QBO influence during boreal summer. ~~This can be seen as consistent with both previous notions: We cannot identify a strong impact of the QBO during boreal summer, but we also did not use the more sophisticated approaches, which might be necessary to detect the signal during boreal summer.~~

4.5.2   Influence of the QBO on the polar stratosphere

The second possible type of interference is the inner-stratospheric influence of the equatorial QBO on the polar winter stratosphere (e.g., Holton and Tan, 1980), which results in the polar winter stratosphere tending to be colder during the QBO westerly phase and warmer during the QBO easterly phase (e.g., Labitzke and van Loon, 1992). This observation is connected to a known influence of the QBO on the occurrence of SSWs during boreal winter (e.g., Camp and Tung, 2007). Hence, both the QBO and the MJO have an influence on the occurrence on SSWs, which have a large influence on the polar MA temperature. Therefore, one reason for the finding that the QBO apparently changes the MJO's influence on MA temperature could be that both influence the occurrence of the SSWs simultaneously with possible interactions or interferences of the effects.

~~We note~~ Note that this QBO effect ~~is so far implicitly~~ would not necessarily remain restricted to the polar winter stratosphere. ~~However, this region is particularly important as it acts as the starting point for the emergence of the IHC pattern (Sect. 4.1). Consistently, it~~ Instead, it has already been shown that the QBO influence on this region also influences other regions of the MA ~~according to~~ via the IHC mechanism (Espy et al., 2011). Moreover, Murphy et al. (2012) show that some details of the IHC mechanism are themselves modified by the QBO phase. Hence, it is plausible that the temperature response to the MJO, which is conveyed by the IHC mechanism, is subject to this QBO influence in the complete MA.

4.5.3   Concluding remarks on the QBO influence

Overall, we cannot discriminate the relative importance of the two possible types of the QBO influence on the MA temperature ~~response~~ signal to the MJO. Whereas a consistency of major aspects can be seen for the QBO influence on the MJO itself (Sect. 4.5.1), we cannot draw any reliable conclusions on the importance of the inner-stratospheric influence (Sect. 4.5.2). This might be possible in the future, when longer datasets allow for a more detailed filtering with respect to other environmental parameters, particularly the exclusion of SSWs.

There is obviously a ~~seasonal~~ hemispheric asymmetry of the QBO influence on the MA temperature response to the MJO (Sects. 3.2 and 3.4)~~: The QBO easterly phase is needed to produce the clearest response pattern during boreal winter, whereas a comparable (although weaker and more noisy) structure is produced during boreal summer in the southern hemisphere regardless of the QBO phase~~. One possible explanation for this apparent asymmetry could be the generally higher variability

of the northern hemisphere boreal winter situation. This might demand for a particularly strong MJO signal to dominate the intraseasonal variability in the northern hemisphere. And the influence of the QBO easterly phase on the MJO during boreal winter could be a major factor to facilitate this strong MJO signal during this season. In contrast, a weaker MJO might already be able to dominate the signal in the more quiescent southern hemisphere, so that a QBO support is not needed to produce the austral winter signal. Another explanation could be the mentioned modification of the occurrence rates of SSWs by the QBO, which is ~~roughly~~ only relevant during boreal winter, because SSWs only rarely happen at all in the southern hemisphere.

4.6 Limitations of the presented analysis

To obtain a complete picture, it will be necessary to study the MJO influence on the MA temperature also with respect to additional environmental conditions, at least the state of the El Niño–Southern Oscillation (ENSO) and the solar 11-year cycle. The length of the analyzed datasets currently limits the number of filters, which can be simultaneously applied, so that we have focused on those influences, which we expected to be most important based on previous research. However, particularly the discrimination of the QBO states based on comparatively only few years of data might be affected by, e.g., the underlying state of the 11-year cycle. ~~As written before, also~~ Also a precise discrimination of boreal winters with and without SSWs is of interest, but also demands for a longer dataset.

Furthermore, we emphasize again the statistical nature of our analysis, which cannot examine the causality and possible physical mechanisms. The present publication aims at making the revealed statistical indications for a connection of the MJO and the IHC already available to the community in order to foster research on the underlying mechanisms. However, to prevent the publication of possible statistical artifacts or spurious correlations, we have embedded our results into previous research, which shows the overall plausibility of a real effect, for which the physical reason can be established in the future.

We note that the statistical approach does also not determine the direction of a physical influence. From the previous literature, it appears ~~likely~~ plausible that an influence at least in the direction from the tropospheric MJO to the MA temperature via an alteration of the wave driving exists. However, possible influences in the opposite direction or feedback loops are not excluded by our study.

5 Summary and conclusions

We have statistically analyzed the connection of the MJO and the MA temperature based purely on observations of MA temperature. We have included all MJO phases in the analysis ~~in order to reveal also the transitions of the MA response when the MJO progresses from one phase to the next. We~~ and have distinguished different ~~environmental conditions, particularly different~~ seasons and states of the QBO. ~~For the sake of brevity, we have focused this paper on zonally averaged data.~~

We have indeed found that the MA temperature is influenced in a statistical sense by the state of the MJO in large areas of the MA and under roughly all considered atmospheric conditions. Still, the strength of the ~~influence~~ signal varies considerably with both the atmospheric conditions and the region of the MA.

Most notably, a pronounced characteristic response pattern, which we called here temporarily "~~five-zone-response~~five-zone-signal", manifested itself under many atmospheric conditions. The first two zones (compare. Fig. 3) are two anomaly areas with opposing sign in the polar winter stratosphere and mesosphere, together constituting a dipole response above the winter pole. These zones show mostly the strongest anomalies among all five zones. A second dipole, comprising the third and fourth zone,
680 is found in the equatorial stratosphere and mesosphere. This dipole has a reversed sign compared to the polar winter dipole. The fifth zone is found above the summer pole in the mesopause region, so that the ~~five-zone-response~~ five-zone-signal spans almost the complete meridional plane. The anomaly of the fifth zone has the same sign as the equatorial mesospheric zone. The overall sign of the complete ~~five-zone-response~~ five-zone-signal is different for different MJO phases. It has been checked with two Monte Carlo approaches that the anomalies of at least these five zones are broadly significant for most analyzed cases.
685 A pattern like the ~~five-zone-response~~ five-zone-signal is known in MA research from a feature called interhemispheric coupling (IHC). This IHC mechanism basically describes, how an initial disturbance in planetary wave drag in the winter stratosphere propagates due to a chain of different dynamical effects through the MA ~~an~~ and thereby causes a similar pattern of temperature disturbances as we have seen here for the MJO ~~influence. More detailed comparisons of the particular locations of the disturbances with the original IHC publications have confirmed the similarity.~~ signals. Moreover, the IHC mechanism
690 works for weak and strong planetary wave activity, causing the one or the other sign of the temperature anomaly pattern as we found it here for different MJO phases.

Hence, one major outcome of the present observational and statistical analysis is the idea that the MJO can ~~lead to the initial planetary wave drag disturbance of the IHC mechanism. The MJO could therefore systematically~~ trigger the IHC ~~mechanism with the one or the other sign, i.e. lead to the initial strengthening or weakening of the planetary wave driving in the winter
695 stratosphere~~pattern in MA temperature. The present study therefore statistically connects an atmospheric feature mostly known in tropospheric research, the MJO, with one mostly known in MA research, the IHC. The MJO as a further potential trigger of the IHC brings new aspects into the research on MA dynamics, since its time scale and periodicity characteristics are quite different from SSWs, which have so far been considered as the starting point ~~of~~ in IHC studies.

The analysis, applied individually to boreal or austral winter data, has revealed that the ~~five-zone-response~~ five-zone-signal
700 appears in both ~~seasons with the response~~ hemispheres with the pattern being roughly mirrored at the equator. The boreal winter ~~response~~ signal is, however, much stronger. Furthermore, the ~~response~~ signal during the boreal winter season shows also a strong dependence on the QBO phase, which we have not convincingly seen for the austral winter. Overall, the strongest anomalies and the clearest spatial ~~pattern~~ patterns appear for boreal winter combined with the QBO easterly phase. In this case, we have found temperature anomalies in the range of $\pm10\,\text{K}$ with the strongest anomalies being located over the winter pole.
705 For austral winter the anomalies are with $\pm3\,\text{K}$ much smaller, but nevertheless, the spatial pattern can easily be identified for most MJO phases.

We also analyzed the change of the MA temperature ~~responses~~ signals while the MJO transitions through its eight phases. For most atmospheric conditions, we could identify a systematic behavior, which is again most clear for boreal winter and QBO easterly conditions. It can be described in two steps: First, the responses to the eight phases can mostly be attributed to either a
710 "weak wave driving" or a "strong wave driving" class according to the sign of the ~~five-zone-response~~five-zone-signal. Second,

for many transitions from one MJO phase to the next a gradual ~~shift of the five-zone-response~~ descent of the five-zone-signal to lower altitudes can be observed, suggesting the MA reacts systematically to each of the MJO phases.

~~We are~~ Although descending patterns are well-known in the polar winter stratosphere, we are not aware of any ~~explicit discussion of such a descent of a~~ discussion of a descending temperature anomaly pattern~~in the literature~~, which is explicitly related to the IHC or the MJO ~~influence on~~ signals in MA temperature. ~~Hence, this is likely a new aspect, for which a mechanism has still to be established. E.g.~~And although large parts of the mechanism behind the descent can probably be explained with already available knowledge, it appears ~~not to be directly clear~~ of interest to clarify in the future whether each phase of the MJO ~~triggers~~ is able to trigger the IHC pattern at a different altitude or if the IHC pattern inherently descends after it has been triggered once by a certain MJO phase or a combination of both.

The results presented here have a statistical character and do therefore not guarantee a real causal connection or uncover the physical mechanism. Particularly, we do not state that a certain MJO phase is the causal reason for the MA temperature pattern, which we obtain for that phase. Since propagation speeds have to be considered in a physical mechanism, it seems more likely that a pattern seen for one MJO phase has been triggered by previous MJO phases. However, by embedding our results in the context of previous research, we have made plausible that a real causal connection as underlying reason ~~is to be expected. This also contains a discussion of the interferences of the found MJO-IHC link with the QBO, SSWs, etc.~~ can be assumed.

~~We note that the present study and the mentioned previous research can benefit from each other. The previous studies provide partly more detailed analyses including physical mechanisms for particular aspects, which supports the plausibility of the current statistical findings. The present study now provides an overarching framework for previously found aspects by identifying the MA temperature response to the MJO as the IHC feature, which spans almost the complete MA.~~

~~We have not attempted to present a physical mechanism together with the statistical results here. Despite the existence of mechanism approaches for individual aspects in the literature, establishing an~~ Establishing an overall mechanism appears to require more extensive future research. Such a mechanism should, in our view, cover at least the following aspects: The nature of the generation of the initial wave disturbance by all MJO phases, the propagation of the signal in both hemispheres as well as in summer and winter, the propagation in the winter hemisphere with and without SSWs, the interaction with the QBO, and the descent of the IHC temperature pattern while the MJO evolves. Of particular interest would be a detailed temporal view on the propagation of the disturbances in the MA that explains, which of the foregoing MJO phases are actually causally responsible for the MA temperature pattern that emerges statistically for a particular MJO phase in our results.

Given that our statistical findings are physically substantiated in the future, we think that the described influence of the MJO on MA temperature is a noteworthy example for the complex couplings across different atmospheric layers and geographical regions in the atmosphere~~: in this case the source of disturbances is located at lower altitudes in the tropics (while it is probably itself influenced from above) and turns out to have observable implications up to 100 altitude and from pole to pole. Moreover, the results further demonstrate the interconnections of different atmospheric features, particularly the MJO, the IHC, the QBO, and SSWs.~~

. Because of the wide coverage of atmospheric regions and included dynamical features, ~~we think that~~ the observational results presented here can be a good benchmark for ~~atmospheric models covering the complete atmosphere. This applies~~

~~particularly for those models, which depend especially on a good representation of troposphere-stratosphere couplings on the intraseasonal timescale, like, e.g., models that are used for intraseasonal~~ the representation of atmospheric couplings in atmospheric models, particularly in the context of intraseasonal weather predictions.

Code and data availability. The releases of the OMI calculation package are freely available from a persistent storage referenced by Hoff-
750 mann (2021), while ongoing improvements are continuously found at https://github.com/cghoffmann/mjoindices, last access August 16, 2022. The MLS temperature data is available for download at https://doi.org/10.5067/Aura/MLS/DATA2520, last access September 15, 2022. NOAA Interpolated Outgoing Longwave Radiation (OLR) data provided by the NOAA PSL, Boulder, Colorado, USA, is available from their web site https://psl.noaa.gov/data/gridded/data.olrcdr.interp.html, last access August 16, 2022. The zonal wind data for the QBO character-ization is provided by Freie Universität Berlin at their website https://www.geo.fu-berlin.de/en/met/ag/strat/produkte/qbo/index.html, last
755 access August 16, 2022.

Author contributions. CGH has outlined the project, performed the analysis and written the manuscript. LGB has carried out a pilot study under the supervision of CGH and CvS showing the potential of the analysis, CvS has extensively discussed the approach and the results during all phases of the project. All authors have reviewed, discussed and improved the manuscript.

Competing interests. The contact author has declared that neither they nor their co-authors have any competing interests.

760 *Acknowledgements.* We would like to thank the two anonymous reviewers for their valuable comments, which helped to improve the paper significantly. This work was supported by the University of Greifswald. We are grateful to the teams of the NASA MLS instrument, of the NOAA OLR dataset, and of the QBO dataset maintained by the Freie Universität Berlin for providing their valuable datasets. The analysis has benefited from discussions on natural variability of the MA temperature and MA dynamics within the DFG (German Research Foundation) research unit VolImpact, particularly within the subproject VolDyn.

References

Allen, D. R., Bevilacqua, R. M., Nedoluha, G. E., Randall, C. E., and Manney, G. L.: Unusual Stratospheric Transport and Mixing during the 2002 Antarctic Winter, Geophys. Res. Lett., 30, 1599, https://doi.org/10.1029/2003GL017117, 2003.

Baldwin, M. P. and Dunkerton, T. J.: Stratospheric Harbingers of Anomalous Weather Regimes, Science, 294, 581–584, https://doi.org/10.1126/science.1063315, 2001.

Baldwin, M. P., Gray, L. J., Dunkerton, T. J., Hamilton, K., Haynes, P. H., Randel, W. J., Holton, J. R., Alexander, M. J., Hirota, I., Horinouchi, T., Jones, D. B. A., Kinnersley, J. S., Marquardt, C., Sato, K., and Takahashi, M.: The Quasi-biennial Oscillation, Rev. Geophys., 39, 179–229, https://doi.org/10.1029/1999RG000073, 2001.

Becker, E. and Fritts, D. C.: Enhanced Gravity-Wave Activity and Interhemispheric Coupling during the MaCWAVE/MIDAS Northern Summer Program 2002, Ann. Geophys., 24, 1175–1188, https://doi.org/10.5194/angeo-24-1175-2006, 2006.

Becker, E. and Schmitz, G.: Climatological Effects of Orography and Land–Sea Heating Contrasts on the Gravity Wave–Driven Circulation of the Mesosphere, J. Atmos. Sci., 60, 103–118, https://doi.org/10.1175/1520-0469(2003)060<0103:CEOOAL>2.0.CO;2, 2003.

Becker, E., Müllemann, A., Lübken, F.-J., Körnich, H., Hoffmann, P., and Rapp, M.: High Rossby-wave Activity in Austral Winter 2002: Modulation of the General Circulation of the MLT during the MaCWAVE/MIDAS Northern Summer Program, Geophys. Res. Lett., 31, L24S03, https://doi.org/10.1029/2004GL019615, 2004.

Beig, G.: Long-Term Trends in the Temperature of the Mesosphere/Lower Thermosphere Region: 1. Anthropogenic Influences, J. Geophys. Res. Space Phys., 116, A00H11, https://doi.org/10.1029/2011JA016646, 2011.

Beig, G., Keckhut, P., Lowe, R. P., Roble, R. G., Mlynczak, M. G., Scheer, J., Fomichev, V. I., Offermann, D., French, W. J. R., Shepherd, M. G., Semenov, A. I., Remsberg, E. E., She, C. Y., Lübken, F. J., Bremer, J., Clemesha, B. R., Stegman, J., Sigernes, F., and Fadnavis, S.: Review of Mesospheric Temperature Trends, Rev. Geophys., 41, 1015, https://doi.org/10.1029/2002RG000121, 2003.

Camp, C. D. and Tung, K.-K.: The Influence of the Solar Cycle and QBO on the Late-Winter Stratospheric Polar Vortex, J. Atmos. Sci., 64, 1267–1283, https://doi.org/10.1175/JAS3883.1, 2007.

Cassou, C.: Intraseasonal Interaction between the Madden–Julian Oscillation and the North Atlantic Oscillation, Nature, 455, 523–527, https://doi.org/10.1038/nature07286, 2008.

Densmore, C. R., Sanabia, E. R., and Barrett, B. S.: QBO Influence on MJO Amplitude over the Maritime Continent: Physical Mechanisms and Seasonality, Mon. Wea. Rev., 147, 389–406, https://doi.org/10.1175/MWR-D-18-0158.1, 2019.

Domeisen, D. I. V., Butler, A. H., Charlton-Perez, A. J., Ayarzagüena, B., Baldwin, M. P., Dunn-Sigouin, E., Furtado, J. C., Garfinkel, C. I., Hitchcock, P., Karpechko, A. Y., Kim, H., Knight, J., Lang, A. L., Lim, E.-P., Marshall, A., Roff, G., Schwartz, C., Simpson, I. R., Son, S.-W., and Taguchi, M.: The Role of the Stratosphere in Subseasonal to Seasonal Prediction: 2. Predictability Arising From Stratosphere-Troposphere Coupling, J. Geophys. Res. Atmos., 125, e2019JD030 923, https://doi.org/10.1029/2019JD030923, 2020.

Espy, P. J., Ochoa Fernández, S., Forkman, P., Murtagh, D., and Stegman, J.: The Role of the QBO in the Inter-Hemispheric Coupling of Summer Mesospheric Temperatures, Atmos. Chem. Phys., 11, 495–502, https://doi.org/10.5194/acp-11-495-2011, 2011.

Garfinkel, C. I., Feldstein, S. B., Waugh, D. W., Yoo, C., and Lee, S.: Observed Connection between Stratospheric Sudden Warmings and the Madden-Julian Oscillation, Geophys. Res. Lett., 39, L18 807, https://doi.org/10.1029/2012GL053144, 2012.

Garfinkel, C. I., Benedict, J. J., and Maloney, E. D.: Impact of the MJO on the Boreal Winter Extratropical Circulation, Geophys. Res. Lett., 41, 6055–6062, https://doi.org/10.1002/2014GL061094, 2014.

Gray, L. J., Beer, J., Geller M., Haigh J. D., Lockwood M., Matthes K., Cubasch U., Fleitmann D., Harrison G., Hood L., Luter-bacher J., Meehl G. A., Shindell D., van Geel B., and White W.: Solar Influences on Climate, Rev. Geophys., 48, RG4001, https://doi.org/10.1029/2009RG000282, 2010.

Haynes, P., Hitchcock, P., Hitchman, M., Yoden, S., Hendon, H., Kiladis, G., Kodera, K., and Simpson, I.: The Influence of the Stratosphere on the Tropical Troposphere, J. Meteorol. Soc. Jpn., 99, 803–845, https://doi.org/10.2151/jmsj.2021-040, 2021.

Henderson, G. R., Barrett, B. S., and M. Lafleur, D.: Arctic Sea Ice and the Madden–Julian Oscillation (MJO), Clim. Dynam., 43, 2185–2196, https://doi.org/10.1007/s00382-013-2043-y, 2014.

Hoffmann, C. G.: Mjoindices: Complete Implementation of the OMI MJO Index Algorithm in Python 3, Zenodo, https://doi.org/10.5281/zenodo.4852196, 2021.

Hoffmann, C. G. and von Savigny, C.: Indications for a Potential Synchronization between the Phase Evolution of the Madden–Julian Oscillation and the Solar 27-Day Cycle, Atmos. Chem. Phys., 19, 4235–4256, https://doi.org/10.5194/acp-19-4235-2019, 2019.

Hoffmann, C. G., Kiladis, G. N., Gehne, M., and von Savigny, C.: A Python Package to Calculate the OLR-Based Index of the Madden-Julian-Oscillation (OMI) in Climate Science and Weather Forecasting, J. Open Res. Softw., 9, 9, https://doi.org/10.5334/jors.331, 2021.

Holton, J. R. and Tan, H.-C.: The Influence of the Equatorial Quasi-Biennial Oscillation on the Global Circulation at 50 {{mb}}, J. Atmos. Sci., 37, 2200–2208, https://doi.org/10.1175/1520-0469(1980)037<2200:TIOTEQ>2.0.CO;2, 1980.

Hood, L. L.: QBO/Solar Modulation of the Boreal Winter Madden-Julian Oscillation: A Prediction for the Coming Solar Minimum, Geophys. Res. Lett., 44, 3849–3857, https://doi.org/10.1002/2017GL072832, 2017.

Jucker, M., Reichler, T., and Waugh, D. W.: How Frequent Are Antarctic Sudden Stratospheric Warmings in Present and Future Climate?, Geophys. Res. Lett., 48, e2021GL093 215, https://doi.org/10.1029/2021GL093215, 2021.

Karlsson, B., Körnich, H., and Gumbel, J.: Evidence for Interhemispheric Stratosphere-Mesosphere Coupling Derived from Noctilucent Cloud Properties, Geophys. Res. Lett., 34, L16 806, https://doi.org/10.1029/2007GL030282, 2007.

Karlsson, B., McLandress, C., and Shepherd, T. G.: Inter-Hemispheric Mesospheric Coupling in a Comprehensive Middle Atmosphere Model, J. Atmos. Sol.-Terr. Phys., 71, 518–530, https://doi.org/10.1016/j.jastp.2008.08.006, 2009a.

Karlsson, B., Randall, C. E., Benze, S., Mills, M., Harvey, V. L., Bailey, S. M., and Russell III, J. M.: Intra-Seasonal Variability of Polar Mesospheric Clouds Due to Inter-Hemispheric Coupling, Geophys. Res. Lett., 36, L16 806, https://doi.org/10.1029/2009GL040348, 2009b.

Kikuchi, K., Wang, B., and Kajikawa, Y.: Bimodal Representation of the Tropical Intraseasonal Oscillation, Clim. Dynam., 38, 1989–2000, https://doi.org/10.1007/s00382-011-1159-1, 2012.

Kiladis, G. N., Dias, J., Straub, K. H., Wheeler, M. C., Tulich, S. N., Kikuchi, K., Weickmann, K. M., and Ventrice, M. J.: A Comparison of OLR and Circulation-Based Indices for Tracking the MJO, Mon. Wea. Rev., 142, 1697–1715, https://doi.org/10.1175/MWR-D-13-00301.1, 2014.

Körnich, H. and Becker, E.: A Simple Model for the Interhemispheric Coupling of the Middle Atmosphere Circulation, Adv. Space. Res., 45, 661–668, https://doi.org/10.1016/j.asr.2009.11.001, 2010.

Kumari, K., Oberheide, J., and Lu, X.: The Tidal Response in the Mesosphere/Lower Thermosphere to the Madden-Julian Oscillation Observed by SABER, Geophys. Res. Lett., 47, e2020GL089 172, https://doi.org/10.1029/2020GL089172, 2020.

Kumari, K., Wu, H., Long, A., Lu, X., and Oberheide, J.: Mechanism Studies of Madden-Julian Oscillation Coupling Into the Mesosphere/Lower Thermosphere Tides Using SABER, MERRA-2, and SD-WACCMX, J. Geophys. Res. Atmos., 126, e2021JD034 595, https://doi.org/10.1029/2021JD034595, 2021.

Labitzke, K. and van Loon, H.: On the Association between the QBO and the Extratropical Stratosphere, J. Atmos. Sol.-Terr. Phys., 54, 1453–1463, https://doi.org/10.1016/0021-9169(92)90152-B, 1992.

Lau, W. K.-M. and Waliser, D. E.: Intraseasonal Variability in the Atmosphere-Ocean Climate System, Springer, Berlin, Heidelberg, 2012.

Liebmann, B. and Smith, C. A.: Description of a Complete (Interpolated) Outgoing Longwave Radiation Dataset, Bull. Amer. Meteor. Soc., 77, 1275–1277, 1996.

Livesey, N. J., Read, W. G., Wagner, P. A., Froidevaux, L., Santee, M. L., Schwartz, M. J., Lambert, A., Millán Valle, L. F., Pumphrey, H. C., Manney, G. L., Fuller, R. A., Jarnot, R. F., Knosp, B. W., and Lay, R. R.: Aura Microwave Limb Sounder (MLS) Version 5.0x Level 2 and 3 Data Quality and Description Document (JPL D-105336 Rev. A), 2020.

Madden, R. A. and Julian, P. R.: Description of Global-Scale Circulation Cells in the Tropics with a 40–50 Day Period, J. Atmos. Sci., 29, 1109–1123, https://doi.org/10.1175/1520-0469(1972)029<1109:DOGSCC>2.0.CO;2, 1972.

Marshall, A. G., Hendon, H. H., Son, S.-W., and Lim, Y.: Impact of the Quasi-Biennial Oscillation on Predictability of the Madden–Julian Oscillation, Clim. Dynam., 49, 1365–1377, https://doi.org/10.1007/s00382-016-3392-0, 2017.

Maycock, A. C., Randel, W. J., Steiner, A. K., Karpechko, A. Y., Christy, J., Saunders, R., Thompson, D. W. J., Zou, C.-Z., Chrysanthou, A., Luke Abraham, N., Akiyoshi, H., Archibald, A. T., Butchart, N., Chipperfield, M., Dameris, M., Deushi, M., Dhomse, S., Di Genova, G., Jöckel, P., Kinnison, D. E., Kirner, O., Ladstädter, F., Michou, M., Morgenstern, O., O'Connor, F., Oman, L., Pitari, G., Plummer, D. A., Revell, L. E., Rozanov, E., Stenke, A., Visioni, D., Yamashita, Y., and Zeng, G.: Revisiting the Mystery of Recent Stratospheric Temperature Trends, Geophys. Res. Lett., 45, 9919–9933, https://doi.org/10.1029/2018GL078035, 2018.

Moss, A. C., Wright, C. J., and Mitchell, N. J.: Does the Madden-Julian Oscillation Modulate Stratospheric Gravity Waves?, Geophys. Res. Lett., 43, 3973–3981, https://doi.org/10.1002/2016GL068498, 2016.

Murphy, D. J., Alexander, S. P., and Vincent, R. A.: Interhemispheric Dynamical Coupling to the Southern Mesosphere and Lower Thermosphere, J. Geophys. Res. Atmos., 117, D08 114, https://doi.org/10.1029/2011JD016865, 2012.

Naujokat, B.: An Update of the Observed Quasi-Biennial Oscillation of the Stratospheric Winds over the Tropics, J. Atmos. Sci., 43, 1873–1877, https://doi.org/10.1175/1520-0469(1986)043<1873:AUOTOQ>2.0.CO;2, 1986.

Randel, W. J., Shine, K. P., Austin, J., Barnett, J., Claud, C., Gillett, N. P., Keckhut, P., Langematz, U., Lin, R., Long, C., Mears, C., Miller, A., Nash, J., Seidel, D. J., Thompson, D. W. J., Wu, F., and Yoden, S.: An Update of Observed Stratospheric Temperature Trends, J. Geophys. Res. Atmos., 114, D02 107, https://doi.org/10.1029/2008JD010421, 2009.

Santer, B. D., Painter, J. F., Bonfils, C., Mears, C. A., Solomon, S., Wigley, T. M. L., Gleckler, P. J., Schmidt, G. A., Doutriaux, C., Gillett, N. P., Taylor, K. E., Thorne, P. W., and Wentz, F. J.: Human and Natural Influences on the Changing Thermal Structure of the Atmosphere, Proc Natl Acad Sci USA, 110, 17 235, https://doi.org/10.1073/pnas.1305332110, 2013.

Schwartz, M., Livesey, N., and Read, W.: MLS/Aura Level 2 Temperature V005, Goddard Earth Sciences Data and Information Services Center (GES DISC), https://doi.org/10.5067/Aura/MLS/DATA2520, 2020.

Schwartz, M. J., Lambert, A., Manney, G. L., Read, W. G., Livesey, N. J., Froidevaux, L., Ao, C. O., Bernath, P. F., Boone, C. D., Cofield, R. E., Daffer, W. H., Drouin, B. J., Fetzer, E. J., Fuller, R. A., Jarnot, R. F., Jiang, J. H., Jiang, Y. B., Knosp, B. W., Krüger, K., Li, J.-L. F., Mlynczak, M. G., Pawson, S., Russell, J. M., Santee, M. L., Snyder, W. V., Stek, P. C., Thurstans, R. P., Tompkins, A. M., Wagner, P. A., Walker, K. A., Waters, J. W., and Wu, D. L.: Validation of the Aura Microwave Limb Sounder Temperature and Geopotential Height Measurements, J. Geophys. Res. Atmos., 113, D15S11, https://doi.org/10.1029/2007JD008783, 2008.

Son, S.-W., Lim, Y., Yoo, C., Hendon, H. H., and Kim, J.: Stratospheric Control of the Madden–Julian Oscillation, J. Climate, 30, 1909–1922, https://doi.org/10.1175/JCLI-D-16-0620.1, 2017.

Sun, C., Yang, C., and Li, T.: Dynamical Influence of the Madden-Julian Oscillation on the Northern Hemisphere Mesosphere during the Boreal Winter, Sci. China Earth Sci., 64, 1254–1266, https://doi.org/10.1007/s11430-020-9779-2, 2021.

Timmreck, C.: Modeling the Climatic Effects of Large Explosive Volcanic Eruptions, WIREs Clim Change, 3, 545–564, https://doi.org/10.1002/wcc.192, 2012.

Tsuchiya, C., Sato, K., Alexander, M. J., and Hoffmann, L.: MJO-related Intraseasonal Variation of Gravity Waves in the Southern Hemisphere Tropical Stratosphere Revealed by High-Resolution AIRS Observations, J. Geophys. Res. Atmos., 121, 7641–7651, https://doi.org/10.1002/2015JD024463, 2016.

von Savigny, C., Rozanov, A., Bovensmann, H., Eichmann, K.-U., Noël, S., Rozanov, V., Sinnhuber, B.-M., Weber, M., Burrows, J. P., and Kaiser, J. W.: The Ozone Hole Breakup in September 2002 as Seen by SCIAMACHY on ENVISAT, J. Atmos. Sci., 62, 721–734, https://doi.org/10.1175/JAS-3328.1, 2005.

Wang, F. and Wang, L.: An Exploration of the Connection between Quasi-Biennial Oscillation and Madden-Julian Oscillation, Environ. Res. Lett., 16, 114 021, https://doi.org/10.1088/1748-9326/ac3031, 2021.

Wang, F., Tian, W., Xie, F., Zhang, J., and Han, Y.: Effect of Madden–Julian Oscillation Occurrence Frequency on the Interannual Variability of Northern Hemisphere Stratospheric Wave Activity in Winter, J. Climate, 31, 5031–5049, https://doi.org/10.1175/JCLI-D-17-0476.1, 2018a.

Wang, S., Ma, D., Sobel, A. H., and Tippett, M. K.: Propagation Characteristics of BSISO Indices, Geophys. Res. Lett., 45, 9934–9943, https://doi.org/10.1029/2018GL078321, 2018b.

Wheeler, M. C. and Hendon, H. H.: An All-Season Real-Time Multivariate MJO Index: Development of an Index for Monitoring and Prediction, Mon. Wea. Rev., 132, 1917–1932, https://doi.org/10.1175/1520-0493(2004)132<1917:AARMMI>2.0.CO;2, 2004.

Yang, C., Li, T., Smith, A. K., and Dou, X.: The Response of the Southern Hemisphere Middle Atmosphere to the Madden–Julian Oscillation during Austral Winter Using the Specified-Dynamics Whole Atmosphere Community Climate Model, J. Climate, 30, 8317–8333, https://doi.org/10.1175/JCLI-D-17-0063.1, 2017.

Yang, C., Smith, A. K., Li, T., and Dou, X.: The Effect of the Madden-Julian Oscillation on the Mesospheric Migrating Diurnal Tide: A Study Using SD-WACCM, Geophys. Res. Lett., 45, 5105–5114, https://doi.org/10.1029/2018GL077956, 2018.

Yang, C., Li, T., Xue, X., Gu, S.-y., Yu, C., and Dou, X.: Response of the Northern Stratosphere to the Madden-Julian Oscillation During Boreal Winter, J. Geophys. Res. Atmos., 124, 5314–5331, https://doi.org/10.1029/2018JD029883, 2019.

Yasui, R., Sato, K., and Miyoshi, Y.: Roles of Rossby Waves, Rossby–Gravity Waves, and Gravity Waves Generated in the Middle Atmosphere for Interhemispheric Coupling, J. Atmos. Sci., 78, 3867–3888, https://doi.org/10.1175/JAS-D-21-0045.1, 2021.

Yoo, C. and Son, S.-W.: Modulation of the Boreal Wintertime Madden-Julian Oscillation by the Stratospheric Quasi-Biennial Oscillation, Geophys. Res. Lett., 43, 1392–1398, https://doi.org/10.1002/2016GL067762, 2016.

Yoo, C., Feldstein, S., and Lee, S.: The Impact of the Madden-Julian Oscillation Trend on the Arctic Amplification of Surface Air Temperature during the 1979–2008 Boreal Winter, Geophys. Res. Lett., 38, L24 804, https://doi.org/10.1029/2011GL049881, 2011.

Yoo, C., Lee, S., and Feldstein, S. B.: Mechanisms of Arctic Surface Air Temperature Change in Response to the Madden–Julian Oscillation, J. Climate, 25, 5777–5790, https://doi.org/10.1175/JCLI-D-11-00566.1, 2012.

Yuan, X., Kaplan, M. R., and Cane, M. A.: The Interconnected Global Climate System—A Review of Tropical–Polar Teleconnections, J. Climate, 31, 5765–5792, https://doi.org/10.1175/JCLI-D-16-0637.1, 2018.

Zhang, C.: Madden-Julian Oscillation, Rev. Geophys., 43, RG2003, https://doi.org/10.1029/2004RG000158, 2005.

Zhang, C.: Madden–Julian Oscillation: Bridging Weather and Climate, Bull. Amer. Meteor. Soc., 94, 1849–1870, https://doi.org/10.1175/BAMS-D-12-00026.1, 2013.

Zhang, C. and Zhang, B.: QBO-MJO Connection, J. Geophys. Res. Atmos., 123, 2957–2967, https://doi.org/10.1002/2017JD028171, 2018.